# Regulation of LDL-cholesterol by circulating PCSK9 and its natural variants

**Alana Renon**

Thesis submitted to the University of Ottawa

In partial fulfillment of the requirements

For the degree of

**Masters of Biochemistry**

Department of Biochemistry, Microbiology, and Immunology

University of Ottawa

Ottawa, Ontario, Canada

## Abstract

Circulating proprotein convertase subtilisin/kexin type-9 (PCSK9) acts as a binding chaperone to mediate endo-lysosomal degradation of cell surface low-density lipoprotein receptor (LDLR)[1]. Gain-of-function (GOF) mutations in *PCSK9* are causative for autosomal dominant hypercholesterolemia (ADH). An acidic intrinsically disordered region (IDR) in the N-terminus of PCSK9's prodomain mediates autoinhibition of LDLR binding, possibly involving an electrostatic intramolecular interaction[2]. Our lab previously showed that contact with hydrophobic membranes triggers the formation of a transient amphipathic α-helix within the IDR required for high-affinity binding of PCSK9 to LDL particles, which antagonizes the PCSK9-LDLR interaction[3]. In a recent collaboration using hydrogen-deuterium exchange/mass spectrometry analysis, we found evidence that the IDR interacts in an aqueous environment with a helical region of the prodomain enriched in positive-charged arginine residues. Interestingly, this region was previously shown to bind heparin sulfate proteoglycans (HSPGs) on the surface of hepatocytes to facilitate the PCSK9-LDLR interaction[4]. An ADH-associated R105W GOF mutation within this helix significantly lowered LDL binding *in vitro*, as did a Y107F substitution to disrupt an intramolecular bond with Asp-129 in an adjacent helix. Multiple amino acid substitutions for Asp-129 abolished PCSK9-LDL binding, including two ADH-associated GOF mutations (D129G[5] and D129N)[1]. Compared to wild-type PCSK9, a PCSK9-D129A variant displayed >3-fold increased binding to purified LDLR extracellular domain and enhanced ability to mediate cell surface LDLR degradation in mouse Hepa1c1c7 hepatoma cells. Thus, like the IDR, the Asp-129 is autoinhibitory of the PCSK9-LDLR interaction. This work supports a model whereby PCSK9's N-terminal acidic IDR contacts basic patches in the prodomain or C-terminal domain under aqueous *versus* hydrophobic conditions, respectively, with the latter allowing LDL to bind at or near Asp-129.

Consequently, LDL binding would mimic the allosteric autoinhibitory effect of the IDR and antagonize the PCSK9-LDLR interaction. Conversely, the binding of PCSK9 to cell surface HSPGs would displace the IDR and mitigate its autoinhibitory effect, thereby promoting PCSK9-LDLR binding and subsequent LDLR degradation in hepatocytes.

## Acknowledgements

I want to express my gratitude to my supervisor, Dr. Thomas Lagace, for his invaluable support and guidance throughout this process. His expert advice and insightful feedback have been instrumental in my development over the past two years. Dr. Lagace provided invaluable hands-on training and consistently understood my demanding student-athlete schedule, offering both flexibility and encouragement. This experience has been profoundly educational, equipping me with numerous techniques that are applicable beyond the lab.

I would also like to thank my thesis advisory committee: Dr. Morgan Fullerton and Dr. Erin Mulvihill for their invaluable insights, guidance, and encouragement throughout my project. Their expertise and feedback were essential in shaping my research.

I would like to extend my appreciation to all members of the Lagace lab, with special thanks to Tanja Kosenko. Tanja was consistently available to answer my questions and provide clarifications on my projects. Her willingness to assist at any time and her thoughtful check-ins during my recovery from injuries were deeply appreciated. Additionally, I am grateful to Ikhuosho Asikhia for his guidance in lab techniques and his help in clarifying protocols and addressing my questions.

Finally, I want to express my heartfelt thanks to my parents. Their unwavering support throughout this journey has been invaluable. I am especially grateful for their patience and willingness to listen to my practice presentations, even when they had little understanding of the content. Their encouragement and presence have been a tremendous source of strength and motivation for me.

# Contents

## Nonstandard Abbreviations and Acronyms Used

| | |
|---|---|
| ADH | Autosomal dominant hypercholesterolemia |
| Apo A /B / C /E | Apolipoprotein A / B / C |
| Apo B48 / ApoB100 | Apolipoprotein B48 or B100 |
| ApoER2 | Apolipoprotein E Receptor 2 |
| ARH | Autosomal recessive hypercholesterolemia |
| BSA | Bovine serum albumin |
| CETP | Cholesteryl Ester Transferase Protein |
| CVD | Cardiovascular Disease |
| Del53-PCSK9 | Delta 53-PCSK9 |
| DMEM | Dulbecco Modified Eagle Medium |
| DNA | Deoxyribonucleic acid |
| dNTP | Deoxynucleotide triphosphate |
| ECD | Extracellular domain |
| EGF-A | Epidermal growth factor-like repeat A |
| ELISA | Enzyme-linked immunosorbent assay |
| ER | Endoplasmic reticulum. |
| FBS | Fetal bovine serum |
| FH | Familial hypercholesterolemia |
| GOF | Gain-of-function |
| HBS-C | HEPES-buffered saline with calcium |
| HDL | High-density lipoprotein |
| HEK293 | Human embryonic kidney immortalized cell line |
| HEK293s | Human embryonic kidney immortalized suspended cell line |
| Hepa1c1c7 | Human hepatoma immortalized liver cell line |
| HMG-CoA | 3-hydroxy-3-methylglutaryl coenzyme A |
| HNF1α | Hepatocyte Nuclear factor 1 alpha |
| HuH7 | Human Hepatoma immortalized cell line |
| HSPG | Heparin-sulfate proteoglycans |

| | |
|---|---|
| IDL | Intermediate density lipoprotein |
| IDR | Intrinsically disordered region |
| INSIG | Insulin-induced gene 1 |
| ITS | Insulin - transferrin - selenium |
| LDL | Low-density lipoprotein |
| LDL-C | Low-density lipoprotein - cholesterol |
| LDLR | Low-density lipoprotein receptor |
| LOF | Loss-of-function |
| LPL | Lipoprotein lipase |
| LPS | Lipopolysaccharide |
| NCLPDS | Newborn calf lipoprotein deficient serum |
| NPC1L1 | Niemann-Pick C1 like 1 |
| OxLDL | Oxidized LDL |
| PACE 4 | Paired basic amino acid-cleaving enzyme 4 |
| PBS | Phosphate buffered saline. |
| PC | Proprotein convertase |
| PCSK9 | Proprotein convertase subtilisin/ kexin type-9 |
| PCSK9i-mAb | PCSK9 inhibitor-monoclonal antibody |
| RNA | Ribonucleic acid |
| S1P / S2P | Site 1 protease / Site 2 protease |
| SCAP | SREBP cleavage activating protein |
| SDS-PAGE | Sodium dodecyl-sulfate - polyacrylamide gel electrophoresis |
| SRE | Sterol regulatory element |
| SREBP | Sterol regulatory element binding protein |
| TAG | Triacylglycerol |
| TBS-C | Tris-buffered saline with calcium |
| TFR | Transferrin receptor |
| TG | Triglycerides |
| VLDL | Very Low-density lipoprotein |
| VLDLR | Very Low-density lipoprotein receptor |

| | |
|---|---|
| WT | Wild type |

**List of Illustrations, figures and tables**

## Chapter 1: Introduction

Proprotein convertase subtilisin kexin type-9 (PCSK9), formerly known as neural apoptosis-regulated convertase-1(NARC1), has recently been identified as playing a key role in cholesterol homeostasis[6]. PCSK9 is a circulating protein that promotes the degradation of cell surface low-density lipoprotein receptors (LDLR) (**Figure 1**). Under normal circumstances, the LDLR binds and mediates endocytic uptake of low-density lipoprotein (LDL), after which the LDLR recycles back to the cell surface. PCSK9 also undergoes endocytic uptake and plasma clearance through binding to the LDLR; however, in this case, the complex undergoes lysosomal degradation, resulting in reduced LDLR present on the cell surface.[4] This reduction leads to decreased clearance of LDL-cholesterol (LDL-c) from circulation, consequently increasing circulating LDL-c levels. Missense mutations in *PCSK9* have been shown to be causative in an autosomal-dominant form of familial hypercholesterolemia (FH), classified as gain-of-function (GOF) due to their association with elevated LDL-c levels[1]. The Lagace lab and others have shown that PCSK9 can also bind to LDL, which inhibits PCSK9 mediated LDLR degradation in cultured hepatic cells[3]. We recently reported that GOF mutations in PCSK9's prodomain and C-terminal domain inhibit LDL binding, such as the S127R and D129G mutations in the prodomain that were shown to abolish LDL binding[1]. However, major unanswered questions remain regarding the exact binding mechanism to LDL and how this inhibits PCSK9's ability to bind LDLR. Therefore, the inhibition of PCSK9 presents a new possibility of therapeutic treatment for FH. This study investigates GOF mutations in the prodomain that interfere with PCSK9-LDL binding, thereby facilitating the characterization of the PCSK9-LDL binding site and further understanding of the interconnection of LDL binding with the PCSK9 prodomain's autoinhibitory effect. Further understanding of PCSK9's autoinhibition could lead to new strategies for the development of therapeutic drugs that inhibit PCSK9 activity by mimicking this natural mode of inhibition.

## 1.1 Hypercholesterolemia:

***1.1.1 Inherited hypercholesterolemia***. Familial hypercholesterolemia (FH) encompasses a collection of inherited genetic abnormalities with autosomal dominant inheritance that result in an increased level of atherogenic low-density lipoprotein (LDL)-cholesterol in the blood. Only one copy of the mutated gene is required to cause the disease and is located on autosomal chromosomes suggesting that both males and females are susceptible. There are two forms of FH: 1) Heterozygous FH and 2) Homozygous FH. Homozygous FH is rare, however, is the most severe form of FH, requiring two defective copies to be inherited while heterozygous FH, the most common form requires a single inherited copy[7]. There are currently three genes in which mutations cause autosomal dominant FH, encoding for LDL receptor (LDLR), apolipoprotein (Apo)B100, and PCSK9, each resulting in lowered plasma clearance of LDL particles via LDLR-mediated endocytosis in the liver[7]. Gene mutations causing defects in PCSK9 function are rare and need to be further investigated.

FH increases the susceptibility of developing atherosclerosis, a cardiovascular disease characterized by the narrowing or thickening of arterial walls due to plaque formation. This condition occurs within the arteries' subendothelial space, ultimately disrupting blood flow in the vessel. Factors contributing to hypercholesterolemia include a high-calorie diet, obesity, and diabetes[7]. The disease initiates with damaged endothelial, which recruits inflammatory factors like adhesion molecules, resulting in increased arterial wall permeability. This increased permeability allows lipid particles (such as LDL) to penetrate the intima, leading to lipid accumulation in the subintima space[8]. LDL accumulates and undergoes oxidative modification induced by vascular smooth muscle cells, forming oxidized LDL (ox-LDL). Ox-LDL acts as a chronic stimulant, promoting endothelial cell recruitment and secretion of molecules that attract monocytes and T-

lymphocytes to the subintima[9]. Monocytes release substances that further damage the endothelium, worsening the inflammation and ox-LDL production. As monocytes and T-cells infiltrate the subintima, monocytes differentiate into macrophages after entering the damaged endothelium, releasing signals that further recruit monocytes to the site[10]. Macrophages engulf ox-LDL via scavenger receptors, becoming foam cells[11]. This process, coupled with ongoing endothelial cell inflammation, continues to attract monocytes and immune cells to the subendothelial space. Foam cells compose the initial atherosclerotic plaque, altering arterial blood flow. As endothelial damage progresses, smooth muscle cells migrate into the vessel lumen and form a fibrous cap around the plaque[12]. The continuous infiltration of foam cells within the plaque results in its necrosis, by enlarging the necrotic core and thinning the fibrous cap, which can lead to the rupture of the plaque causing thrombosis[10].

By reason that FH is associated with decreased LDL clearance, this naturally leads to increased plasma LDL binding to the arterial intima's proteoglycans[12]. This interaction augments endothelial permeability and increases lipoprotein binding molecule expression within the plaque, further retaining LDL and ultimately commencing the initial steps of atherosclerosis development.[12] Therefore, LDL-c lowering treatment in FH reduces the development of atherosclerosis or prevents atherosclerosis by targeting the LDLR, apoB, or PCSK9 gene expression[7].

***1.1.2 PCSK9 in FH***. Recent discoveries have revealed that PCSK9 plays a critical role in cholesterol metabolism, specifically in the LDL receptor (LDLR) degradation, and in 2003, it was identified as the third locus involved in autosomal-dominant FH[13]. The LDLR, a cell surface protein, plays a critical role in LDL uptake and is highly expressed in liver hepatocytes and adrenal

cells. However, GOF mutations in PCSK9 can result in enhanced LDLR binding promoting degradation of the LDLR and preventing clearance of LDL-c from circulation. These GOF mutations in PCSK9 are associated with FH by either enhancing LDLR degradation or inhibiting/preventing PCSK9-LDL binding, leading to enhanced levels of circulating LDL-C[14]. As an example, a well-characterized GOF mutation is D374Y in PCSK9's catalytic domain which increases LDLR-binding affinity by >10-fold, leading to higher levels of LDLR degradation and an increase in circulating LDL-c levels[1].

Conversely, loss of function (LOF) mutations in *PCSK9* lead to lower levels of circulating LDL, thereby having a protective cardiovascular effect and protection against the development of hypercholesterolemia[14]. Some LOF mutations are relatively common among certain ethnic groups, for instance, R46L occurring in 3% of European Caucasians and C679X occurring in 2% of African Americans [15]. Previous studies have shown that the LOF mutations can cause a decrease between 15% and 28% in LDL-cholesterol levels[16]. For example, the R46L LOF mutation in PCSK9 was associated with a ≥15 mg/dL lower LDL-C levels and a 47% reduction in developing cardiovascular disease[17]. The discovery of LOF mutations within PCSK9 provided additional impetus for the development of PCSK9 inhibitors to lower PCSK9 activity and reduce LDL-c levels. As well, the R46L LOF mutation in PCSK9 attenuates PCSK9 activity seemingly without impacting other biological processes in the body.[16] The discovery of a connection between PCSK9 and plasma LDL-c levels has made PCSK9 a key component in drug targeting to treat and prevent cardiovascular diseases.

***1.1.3 Statins.*** Statins are the standard therapy to treat hypercholesteremia and FH, acting by inhibiting hydroxymethylglutaryl-CoA (HMG-CoA) reductase, the rate-limiting enzyme in *de novo* cholesterol synthesis. By inhibiting cholesterol synthesis, statins reduce the hepatocyte cholesterol content, thereby activating the cholesterol-responsive transcription factor sterol regulatory element-binding protein 2 (SREBP-2), raising LDLR gene and protein expression and increasing LDL-c clearance from circulation[20]. Statins can lower LDL-c levels up to 60%. However, statin intervention is associated with multiple side effects and intolerability in some patients[18], while others receiving a tolerable amount of statins may fail to meet the target range of LDL-c levels and may experience coronary events[19]. The most common side effects of statins are myopathies, hepatotoxicity, and diabetes mellitus[19]. About 15%-20% of patients appear to be statin resistant, meaning despite taking a drug designed to lower cholesterol levels, the patients fail to reduce cholesterol levels[20]. Genetic factors, diet, lifestyle, or the interaction of statins with other molecules can cause this resistance. Some individuals with FH have higher baseline cholesterol levels from which statins may not be sufficient to reduce cholesterol within the normal range[20]. Studies have shown that the recombinant treatment consisting of a tolerable dose of statins alongside other treatments such as PCSK9 monoclonal antibodies or ezetimibe further decreases LDL-c levels in patients presenting with statin resistance[20].

Statin treatment is effective by inhibiting HMG-CoA reductase; however, this inhibition activates SREBP2 transcriptional factors which are triggered by low intracellular cholesterol levels[21]. SREBP2 simulates the activation of LDLR-expressing genes, increasing the LDLR present on the cell surface resulting in an increased clearance of LDL-c. However, the activation of SREBP2 also activates the transcription of PCSK9 possibly creating a futile cycle[22]. Ultimately, statins decrease

cholesterol levels but, the increased transcription of PCSK9 restricts their effectiveness[22]. Thus, the inhibition of PCSK9 would elevate the expression of the LDLR induced by statins, resulting in an enhanced clearance of LDL-c, improving the effectiveness of statins.

***1.1.4 PCSK9 targeting in cholesterol lowering therapies.*** Since the discovery of PCSK9, many new treatments have been developed. The molecular mapping of the PCSK9-LDLR binding interface allowed the development of therapeutic PCSK9 inhibitory monoclonal antibodies (PCSK9i-mAbs) that bind to PCSK9 and block it from interacting with the LDLR by blocking PCSK9's interaction with the epidermal growth factor-like (EGF)-A domain of LDLR[23]. Two of these therapies have been approved for use in patients to treat hypercholesterolemia: alirocumab and evolocumab. PCSK9i-mAb therapy also exerts beneficial effects on inflammation and immune cell function independent of LDL lowering, although the underlying mechanism(s) remain unknown [24]. One possibility is that PCSK9 can also bind to EGF-like domains in other proteins and PCSK9i-mAbs would also block these interactions[24]. However, the high cost of PCSK9i-mAb therapies (~$15,000/patient/year)[25] limits their usage, especially in treating chronic conditions such as hypercholesterolemia (**Fig. 1**)[18]. Another recent treatment is Ezetimibe, an oral medication used to treat hypercholesterolemia. Ezetimibe inhibits dietary cholesterol absorption at the brush border of enterocytes carried by the sterol transporter Niemann-Pick C1 like 1(NPC1L1). This decreases the absorption of cholesterol from the diet. However, Ezetimibe is less effective on its own reducing LDL-c levels by 15-20% and is usually used in conjunction with statins[26].

Other treatments aimed at inhibiting PCSK9 activity are at different stages within the developmental pipeline, such as nucleic acid drugs and small molecules. Inclisiran is a small-

interfering RNA therapy approved in 2020 that lowers PCSK9 expression in the liver, thereby increasing the expression of the LDLR on the cell surface of hepatocytes and increasing LDL-c clearance[27]. However, inclisiran is injected subcutaneously possibly causing injection site infections and the activity of inclisiran lasts 6 months without any opportunity of intervening or stopping its effects[27]. In addition, this treatment will only affect liver-derived PCSK9, while other sites in the body also produce PCSK9. Current small molecule drug approaches aim to target the PCSK9-LDLR binding interface in the same strategy as PCSK9i-mAbs but in a more cost-effective manner; however, the binding interface is largely flat and without obvious binding pockets[23]. Therefore, once bound to PCSK9, these inhibitors could be more susceptible to dissociation[28]. Further understanding the structural dynamics and binding properties of PCSK9 could allow an alternative discovery of PCSK9 inhibitory strategies for economical and effective LDL-c lowering therapies.

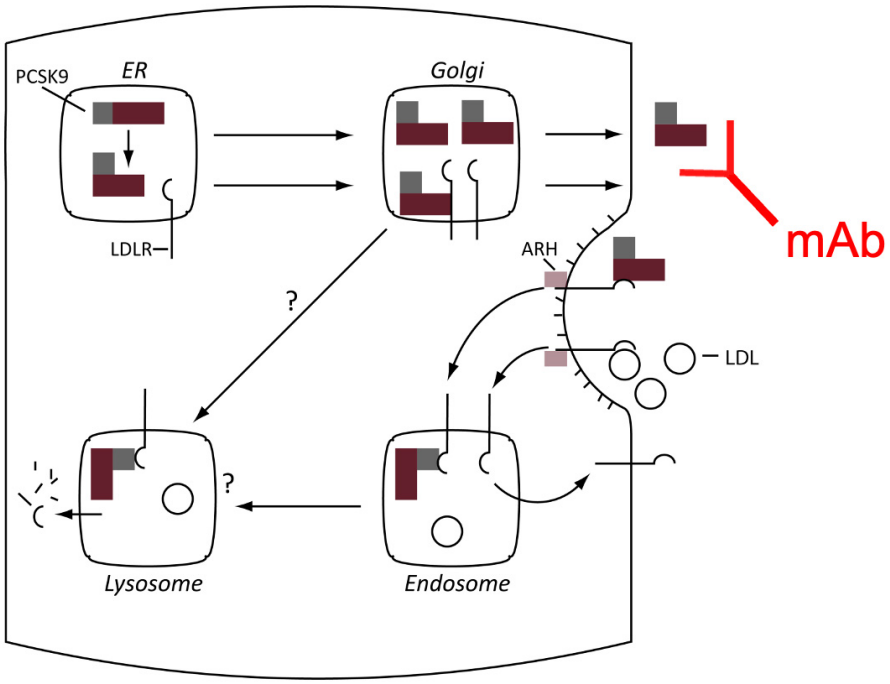


**Figure 1: The outlined process of PCSK9-mediated LDLR degradation and the action of PCSK9 inhibitory (PCSK9i) monoclonal antibodies (mAbs).** The LDLR is synthesized in the ER, matures in the Golgi, and moves to the cell surface to bind LDL with the help of adapter protein ARH[29]. After internalization of the complex, the acidic environment of the endosome causes the dissociation of the LDLR-LDL complex, allowing the LDLR to be recycled to the cell surface while LDL is directed to the lysosome for degradation. PCSK9 is synthesized and autocleaved in the ER, matures in the Golgi and is secreted into circulation. Once bound PCSK9 is internalized with the LDLR (via ARH), the acidic endosome strengthens the bond, leading both to lysosomal degradation. However, PCSK9i-mAbs bind to PCSK9 and block its interaction with LDLR, thus preventing LDLR degradation and promoting its recycling, lowering cholesterol levels.

## 1.2 PCSK9: A member of the proprotein convertase family

***1.2.1 Proprotein Convertases.*** Proprotein convertases (PCs ) are serine proteases that exhibit structural similarities to bacterial subtilisin and kexin found in yeast. PCs play an important role in the activation of various proteins by cleaving them at specific sites, triggering the activation, inactivation, or functional changes in proteins such as growth factors and hormones[30]. The mammalian PC family is composed of nine members: PC1, PC2, Furin, PC4, PC5, PACE4, PC7, SKI-1/S1P (subtilisin kexin isozyme 1 or S1P), and PCSK9, each having distinct roles[31]. The nine PCs are expressed in various tissues, except for PC7, SKI-1, and furin, which all are universally expressed. PC1 and PC2 are predominantly implicated in regulatory pathways involved in endocrine and neuronal cells[32], whereas PC4 is found in the placenta and gonads and PACE4 in the muscles, heart, pituitary kidneys, and cerebellum. PC5 is present in the intestines, kidneys, and ovaries, while PCSK9 is expressed in the liver, kidneys, and intestines[33 34]. Each member of the PC family serves a specific function, with SKI-1 and PCSK9, for example, playing an important role in cholesterol and fatty acid metabolism[35].

All PCs share the same general structure: a signal sequence followed by a prodomain, a conserved subtilisin-like catalytic domain, and a C-terminal domain. The PCs are synthesized as inactive precursors, with post-translational modifications being necessary to create the mature form, the first being an autocatalytic cleavage in the endoplasmic reticulum (ER)[30]. This event causes the release of the prodomain, which remains bound to the catalytic domain, rendering it inactive. The prodomain serves a dual function; it acts as a chaperone to inhibit the catalytic domain and assists in the proper folding of the protein. PCSK9 and S1P are cleaved at non-basic residues, while the other members are cleaved at basic residues in the (R/K)Xn (R/K)↓ motif[36]. Most PCs undergo a

second proteolytic cleavage in the prodomain that relieves the inhibition and exposes the catalytic site, activating the protein[37]. However, PCSK9 does not undergo a second autocleavage, remaining inactive[30].

***1.2.2 PCSK9.*** As its name signifies, PCSK9 is the ninth member of the mammalian PC family of serine endoproteases. Human PCSK9 is a 692-amino acid protein composed of a signal sequence (aa 1-30), a prodomain (aa 31–152), a catalytic domain (aa 153–454), and cysteine-histidine rich (CHR) C-terminal domain (aa 455–692) (Fig. 2)[38]. The prodomain of PCSK9 contains an N-terminal intrinsically disordered region (IDR; aa 31-60) along with two alpha-helices and four-stranded antiparallel β-sheets. The last β-sheet forms a junction with the catalytic domain, extending into the catalytic site to block substrate access[39]. It was discovered that a PCSK9 variant with the removal of the first twenty-one amino acids in the prodomain (Δ31-52, referred to hereafter as del53-PCSK9) displayed >7-fold increased binding affinity to LDLR despite being far removed from the binding interface to EGF-A (**Figure 2**)[13]. This indicates that the prodomain IDR plays an autoinhibitory role in PCSK9's ability to bind LDLR[2]. The catalytic domain is responsible for interacting with the EGF-A domain of the LDLR. The D374 residue of the PCSK9 catalytic domain forms a hydrogen bond with H306 of the EGFA in the LDLR, with the D374Y GOF mutation improving this bonding interaction[39]. The C-terminal domain of PCSK9 consists of a disordered region forming three tandem repeats referred to as M1, M2, and M3 that are made up of six antiparallel β-strands. The β-strands are held together by three internal disulfide bonds[39]. The M2 domain is enriched in histidine residues, which could influence a pH-dependent increase in the binding affinity of PCSK9 to LDLR[40], likely a key determinant of PCSK9's ability to maintain binding to LDLR in acidic early endosomes and mediate LDLR degradation[41]. Deletion

of the C-terminus negatively affects PCSK9 secretion, suggesting an important role in processing/maturation[42]. PCSK9 undergoes several post-translational modifications, namely two phosphorylations (serine 47 and 699), N-glycosylation (asparagine 533), and sulfation (tyrosine 38)[43]. There is evidence that phosphorylation may protect PCSK9 from proteolysis; however, none of these post-translational modifications are required for PCSK9 activity[13].

PCSK9 is mainly produced in liver hepatocytes and is secreted into the circulation. Similar to other PCs, during its maturation, the prodomain (14 kDa) is removed from the rest of the protein (60 kDa) in the ER through autocatalytic cleavage[6]. Human PCSK9 is autocleaved at the $\mathit{V}$FA$\mathit{Q}_{152}\downarrow$ [39]. Mutations in this area, such as the LOF mutation Q152H, prevent proper cleavage, preventing its secretion[44]. The cleaved prodomain remains non-covalently bound to the catalytic domain (60 kDa), blocking the active site and rendering it inactive[45] [46]. The autocleavage process of the PCSK9 prodomain is necessary for its exit from the ER into circulation[47] (**Figure 1**). Unlike other PCs, no secondary cleavage of the PCSK9 prodomain occurs and therefore the mature enzyme remains in its inactive form[30]. PCSK9 is prone to proteolysis by furin, also known as PC3. Approximately 10–20% of PCSK9 in human plasma is furin-cleaved[54]. Furin cleaves PCSK9 at position R218 located in the catalytic domain, generating a truncated form of PCSK9 that is inactive for binding to LDLR[48]. Since its discovery and initial characterization in 2003, there has been an increased understanding of the key role that PCSK9 plays in cholesterol metabolism through its ability to mediate hepatic LDLR degradation[49]

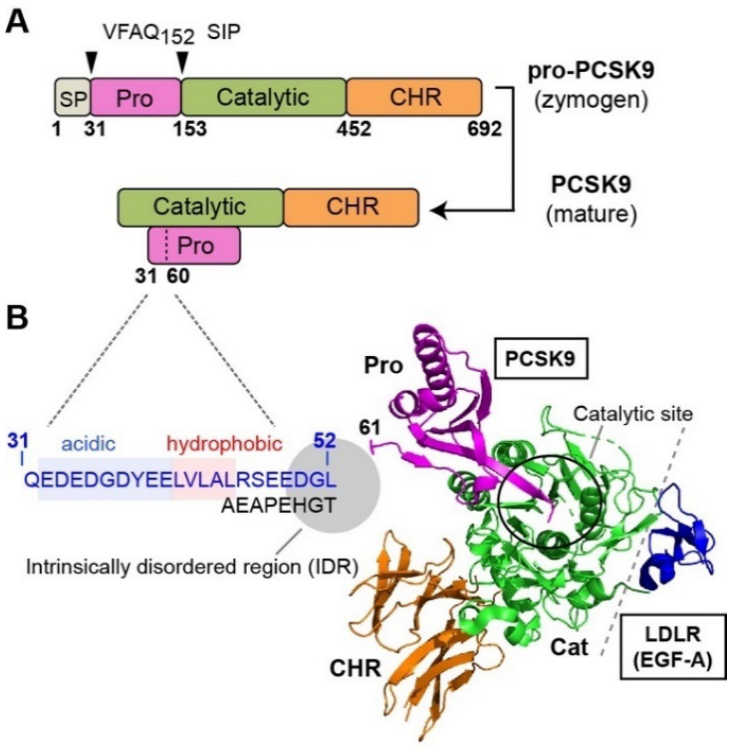


**Figure 2: Representation of PCSK9 structure.** A) A pro-PCSK9 composed of a signal peptide, a prodomain, a catalytic domain and a C-terminus is shown alongside mature PCSK9. The mature PCSK9 has the prodomain noncovalently bound to the catalytic domain blocking its active site. The autocleavage site is shown on the pro-PCSK9 as well as the amino acid sequence of the intrinsically disordered region in PCSK9s prodomain. B) a co-crystal structure showing the PCSK9-LDLR binding interaction. PCSK9 prodomain is represented in purple. The catalytic domain of PCSK9 (green) is seen interacting with the EGFA domain of the LDLR (blue)[1]**.** Protein crystal structure by **Kwon et al, 2008**[23].

## 1.3 PCSK9 as a regulator of the LDLR

***1.3.1 LDLR degradation.*** LDLR is a modular protein consisting of a ligand-binding domain composed of seven cysteine-rich repeats (R1-R7, also known as L1-L7), an epidermal growth

factor (EGF) precursor homology domain composed of two EGF-like repeats (EGF-A and EGF-B) separated from a third EGF-like repeat (EGF-C) by a beta-propeller region, an O-linked sugar domain, a transmembrane domain, and a short cytoplasmic tail region[50](**Figure 3**). Genetic defects found throughout the LDLR sequence causing a loss-of-function (LOF) result in FH, in which there is an accumulation of LDL-cholesterol (LDL-c) in the blood. The LDLR has two relationships that affect cholesterol homeostasis: 1) it's binding to LDL, and 2) it's binding to PCSK9[17].

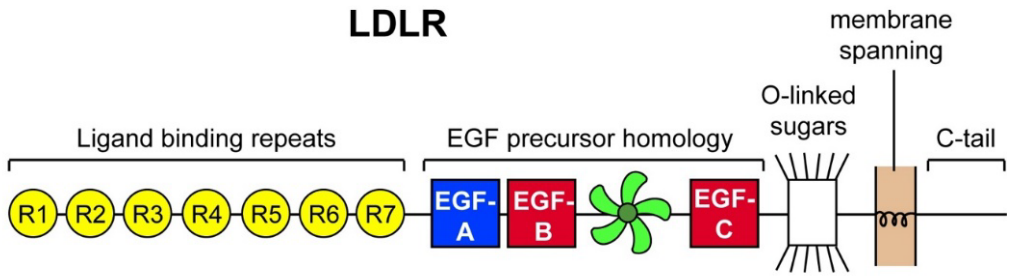


**Figure 3: The structure of the LDLR**. The key domains of the LDLR are highlighted: the ligand binding repeats (R1-R7), the EGF precursor homologue domain (EGF-A, B, C), the O-linked sugars and the C-tail.

LDLR traffics to the cell surface where it plays a critical role in LDL uptake, with the highest expression in liver hepatocytes and adrenal cells. The N-terminal ligand binding domain is composed of seven cysteine-rich repeats, and binds to the apoB100 protein component of LDL, with each LDLR able to bind one apoB100 molecule at a time[50]. At neutral pH, the LDLR adopts an elongated "open" conformation, revealing the ligand binding domain[50]. Once LDL-apoB100

binds to LDLR, the complex is internalized by the cell through clathrin-mediated endocytosis[50]. Following internalization, a pH-dependent switch occurs causing the LDLR to adopt a "closed" conformation in which the ligand binding domain forms an intramolecular interaction with the beta-propeller domain[50]. This allows the release of LDL particles after which the LDLR is recycled to the cell surface where it is again available to capture an LDL particle[50] (**Figure 1**). Meanwhile, the released LDL travels to lysosomes, where it is degraded, releasing cholesterol, fatty acids, phospholipids, and amino acids for use in cell metabolism[50]. Apolipoprotein E (apo E), found in lipoproteins such as chylomicrons, VLDL, IDL, and HDL, also serves as a ligand for LDLR[17]. Similar to apoB100, apoE also releases from LDLR in acidic early endosomes[44]. However, PCSK9 binds tighter to LDLR at acidic pH, leading to the degradation of both proteins in the lysosome instead of LDLR being recycled to the cell surface[1].

Hepatic LDLR expression is regulated at many levels in the cell, one of which is through the transcription factor SREBP-2[51]. SREBP-2 is initially synthesized as an inactive membrane-bound precursor in the ER[51]. In the presence of low cholesterol levels, the polytopic ER membrane protein SCAP dissociates from INSIG, another ER-membrane protein, and SCAP then enters vesicles to transport with bound SREBP2 from the ER to the Golgi apparatus[52]. At the Golgi, SREBP-2 is sequentially cleaved by two proteases, Site-1 protease (S1P) and Site-2 protease (S2P), releasing the soluble active form of SREBP2[52]. The transcriptional factor then translocates to the nucleus to bind to the sterol regulatory element (SRE) within the promoter region of target genes mainly involved in cholesterol biosynthesis, but also that of LDLR involved in cholesterol uptake in the form of LDL-c[44]. Since statin drugs act to lower cell cholesterol levels by inhibiting cholesterol synthesis, this in turn activates SREBP-2 leading to increased transcription of the

LDLR gene, increased LDLR protein expression at the cell surface, and increased clearance of plasma LDL-c[51].

***1.3.2 PCSK9-LDLR binding.*** PCSK9 plays a role in cholesterol homeostasis by binding to LDLR and targeting the receptor for lysosomal degradation, reducing LDLR levels. Importantly, PCSK9 catalytic activity is not required for LDLR binding; instead, it acts as a chaperone, leading LDLR to lysosomal degradation[53]. The exact mechanism of PCSK9-mediated LDLR degradation remains unknown. The catalytic domain of PCSK9 binds to the EGF-A domain of the LDLR in a calcium-dependent manner, specifically encompassing amino acids 153–384 on PCSK9. Once bound, the PCSK9-LDLR complex undergoes endocytosis[53]. Unlike the LDL-LDLR complex, PCSK9's binding interaction with the LDLR is strengthened at acidic pH, so PCSK9 remains tightly bound in early endosomes, preventing the LDLR from being recycled and redirecting the receptor for lysosomal degradation[41] (**Figure 1**). It has been proposed that PCSK9 binding to the LDLR holds the receptor in an extended conformation, preventing the acid-dependent "closed" conformation of the LDLR required for its efficient recycling[48]. Alternatively, or in addition, PCSK9 may bind to accessory proteins that reroute the LDLR towards lysosomes, the so-called "Protein X" theory (**Figure 4**)[54]. The introduction of D374Y GOF enhances the affinity for the LDLR[55], further demonstrating the involvement of the PCSK9 catalytic domain in binding, specifically through the interaction of the D374 residue with the EGF-A domain [41]. The D374 residue on the surface of the PCSK9 catalytic domain binds the H306 residue of the LDLR EGF-A[23]. Other key contacts include a hydrophobic interaction involving F379 of PCSK9 with L318 of EGF-A, and R196 of PCSK9 forming a salt bridge with D310 of EGF-A[23]. The EGF-A domain of the LDLR forms no interactions with PCSK9's prodomain or C-terminal domain. In addition to the primary binding interaction between the catalytic domain of PCSK9 and the EGF-A domain of the LDLR, the

prodomain of PCSK9 can form van der Waals interactions with the beta-propeller of the LDLR, which may assist in the degradation process by creating a second point of contact[54] (Figure 3). The binding in the prodomain and the catalytic domain of PCSK9 could potentially inhibit the LDLR from adopting a closed conformation, resulting in its inability to be recycled onto the cell surface[48]. As well, the C-terminus of PCSK9 may interact with the ligand binding repeats of the LDLR, further strengthening the binding between PCSK9 and the LDLR[48]. In addition, there are molecules on the cell surface, heparan sulfate proteoglycan (HSPG), which help present PCSK9 to the LDLR, facilitating this interaction. The HSPGs recognize an arginine-rich loop located in the PCSK9 prodomain[56]. LOF mutations in this area, such as R93C, are thought to decrease HSPG binding, resulting in lower LDLR binding[56].

It has also been discovered that PCSK9 can bind to other members of the LDLR family, such as apolipoprotein E receptor 2 (ApoER2) and VLDLR, but with less affinity than the LDLR[57]. Replacing the EGF-A domain of the VLDLR with that of the LDLR increased the degradation of the VLDLR[58]. Sequencing of the EGF-A domain present in the members of the LDLR family revealed the amino acids are conserved. However, a leucine residue (L318) identified as critical for binding to the F379 residue of PCSK9 is only present in the EGF-A domain of the LDLR, suggesting it may play a critical role in PCSK9 binding[50 53]. The replacement of aspartic acid for leucine in the EGF-A domain of the LDLR, so it resembles the EGF-A domain of the VLDLR, reduces PCSK9 binding significantly[59]. This suggests that the LDLR contains specific amino acids critical for PCSK9 binding.

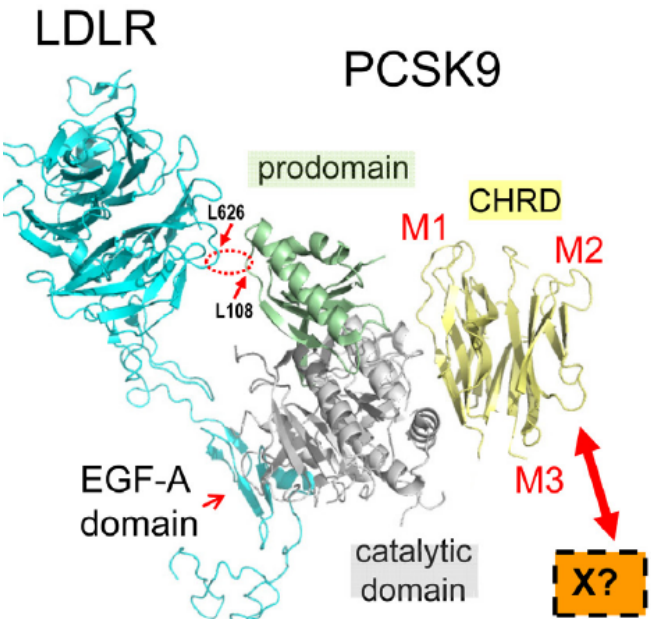


**Figure 4: Overview of PCSK9's binding to the LDLR**. The X-ray crystal structure of PCSK9 demonstrates its prodomain in green, catalytic domain in grey and the C-terminus in yellow. The catalytic domain of PCSK9 binds to the EGF-A domain of the LDLR. PCSK9 prodomain is in proximity to the LDLR b-propeller and forms van der Waal interactions, creating a second point of contact in the PCSK9-LDLR interaction[60]. It's hypothesized that an interaction between M2 and a membrane protein (in this case protein X) assists in guiding the complex to the lysosome for degradation[40]. This protein structure was modelled by **Seidah et al, 2014[60].**

## 1.4 Regulation of circulating PCSK9 levels

***1.4.1 Transcriptional regulation.*** As mentioned above, the transcription factor SREBP-2 regulates all genes necessary for cholesterol synthesis and is activated by depletion of cell membrane cholesterol and is translocated to the nucleus[51]. This results in the increased transcription of certain genes, such as the LDLR, along with those involved in cholesterol biosynthesis[24]. Interestingly,

PCSK9 was found to also be regulated by SREBP-2[61]. This suggests a potential futile cycle of LDLR production and PCSK9-mediated degradation when SREBP-2 is activated[62]. However, since plasma LDL-c levels in humans remain relatively steady and PCSK9 levels fluctuate widely, post-transcriptional mechanisms likely exist to limit PCSK9-mediated LDLR degradation[63]. One such mechanism could be through binding to plasma LDL, which would have an inhibitory effect on PCSK9, reducing its ability to bind to the LDLR[63]. PCSK9 can bind simultaneously to LDL and LDLR, as the binding location for each is situated in a different region of PCSK9[64].

PCSK9 levels in plasma decrease with fasting and increase postprandially, suggesting that PCSK9 has a temporary role in intestinal and hepatic lipoprotein production and the fasting-feeding cycle[65]. Since PCSK9 levels are higher in the postprandial state, a greater percentage of PCSK9 could be unbound to LDL and thereby more active, leading to increased hepatic LDLR degradation[54]. Since PCSK9 function presumably evolved in a low-nutrient environment, this may have served an important role in preventing excessive uptake of VLDL and chylomicron remnant lipoproteins that contained the LDLR ligand apoE. In this way, these triglyceride-rich lipoproteins would remain in circulation longer for delivery of fatty acids to peripheral tissues[54]. The VLDL remnants that remain in circulation are further metabolized to IDL and then to LDL[43]. Thus, PCSK9 action would not only lower LDL-c clearance but could also increase LDL production from the precursor VLDL, leading in the two fashions to cause LDL-c accumulation in the plasma[54]. Eventually, during the fasting period, as PCSK9 concentration falls and LDL increases, more PCSK9 will be LDL-bound and inactive, allowing for improved LDL-c clearance from the plasma[66] **(Figure 7)**. This negative feedback model suggests that LDL plays a large role in cholesterol homeostasis, not only through the delivery of cholesterol to tissues but also through

the regulation of PCSK9 activity[54]. PCSK9 should be able to sense the levels of LDL-c in plasma, which in turn would direct it to either bind to LDL or the LDLR.

Another promoter element that has been identified to regulate PCSK9 transcription is that which binds the transcription factor hepatocyte nuclear factor 1 (HNF1α), known to regulate the expression of genes in the intestine and the liver in response to acute inflammation in addition to other stimuli[67] [68]. Together, HNF1α and SREBP2 collaborate to regulate PCSK9 transcription. Increased HNF1α activity in hamsters' livers promoted PCSK9-mediated LDLR degradation that overrode the positive effect of statins on the LDLR mRNA expression[69]. As well, mutations observed in the HNF1α promoter reduced PCSK9 expression, suggesting that HNF1α impacts PCSK9 expression[43].

## 1.5 PCSK9 and lipoproteins.

***1.5.1 Lipoproteins.*** Lipoproteins transport hydrophobic lipids such as cholesterol and triglycerides in circulation since they are insoluble in water[70]. Their structure is composed of a hydrophobic lipid core composed of triglycerides and cholesteryl esters, an outer membrane composed mainly of phospholipids, and associated apolipoproteins[70]. The phospholipids are amphipathic, with their hydrophobic tails facing the hydrophobic inner core and their polar heads facing the external environment, thus the external membrane of lipoproteins is a single layer rather than a bilayer[70]. Lipoproteins can be classified into various groups based on size, density, associated apolipoproteins, and lipid composition[71]. The main lipoproteins are chylomicrons, very low-density lipoproteins (VLDL), intermediate-density lipoproteins (IDL), low-density lipoproteins (LDL), and high-density lipoproteins (HDL)[71]. There are two main pathways for lipoprotein

synthesis: exogenous (diet–packaged in the intestine) and endogenous (synthesized by the liver) (**Fig. 5**)[72].

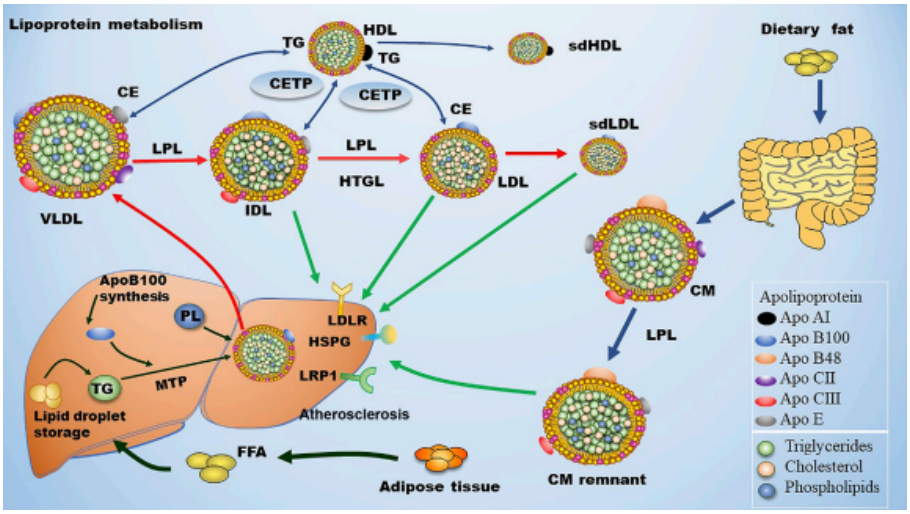


**Figure 5: Overview of lipoprotein metabolism.** Chylomicrons are assembled in enterocytes from triglycerides and cholesterol received from the diet. As chylomicrons circulate, they release fatty acids through triglycerides hydrolyzed by lipoprotein lipases forming chylomicron remnants. The liver produces triglyceride-rich VLDL which are also metabolized by lipoprotein lipases by peripheral tissues forming IDL and eventually LDL[72]. HDL donates cholesterol esters to VLDL and LDL in exchange for triglycerides through the action of cholesterol ester transfer protein (CETP)[73]. This diagram was designed by **Qiao et al, 2022**[73]**.**

The large and least dense chylomicrons are packed with dietary lipids in the small intestine, holding triglycerides in their core. Chylomicrons are metabolized in circulation by lipoprotein lipases releasing fatty acids for uptake in peripheral tissues and forming chylomicrons remnants[72]. Chylomicron remnants circulate back to the liver where they are taken up by a receptor's recognition of apolipoprotein E (apo E)[71]. The liver synthesizes VLDL which are enriched in

triglycerides. Similarly to chylomicrons, VLDL's role is to transport triglycerides from the liver to peripheral tissues[73]. As VLDLs circulate they lose triglycerides through hydrolysis by lipases, forming the short-lived IDL and eventually cholesterol-rich LDL, which can distribute cholesterol to peripheral tissues through the binding of apoB100 with the LDLR[72]. Since the liver has high LDLR expression, most LDL is eventually recycled back to the liver[74]. Lipoprotein[a] (Lp[a]) is another lipoprotein in circulation that could transport cholesterol. Lp[a] structurally resembles LDL but with a key difference, specifically, the apoB100 is covalently bound by a disulfide bond to apolipoprotein[a] (apo[a]), a protein that resembles plasminogen[75]. The exact role of Lp[a] is not well understood, but it is known to be atherogenic since it transports oxidized phospholipids[75]. The reverse transport of cholesterol from peripheral tissues to the liver is performed by HDL to produce bile or lipoproteins[76]. The loss of cholesterol as bile within the feces is the only means of the body to remove excess cholesterol since cholesterol cannot be broken down enzymatically. "Empty" HDL circulate and collects excess cholesterol from peripheral tissues for return to the liver. HDL can also exchange cholesterol for triglycerides through CETP with VLDL and LDL[71]. Thus, the overall effect of HDL is atheroprotective (**Fig. 5**)[71].

***1.5.2 Apolipoproteins.*** Apolipoproteins are found on the surface of lipoproteins. They are responsible for binding lipoproteins to the receptors on the target tissue and can affect lipoprotein metabolism by lipases[72]. Mutations in apolipoproteins often lead to disease; for instance, mutations in apoB100 are implicated in FH. The important apolipoproteins are apoE, apoAI, apoAII, apoAIV, apoCI, apoCII, apoB48 and apoB100[72]. Apolipoprotein composition is used to classify lipoproteins, as different apolipoproteins are found on various lipoproteins, each serving distinct functions[72]. A principal function of apolipoproteins involves serving as ligands for binding with

receptors on target cells, such as apoB100 and apoE recognition by the LDLR[71]. Apolipoproteins can also have roles as cofactors for enzymes, for instance, lipoprotein lipase requires the presence of apoCII to hydrolyze chylomicron and VLDL triglycerides[77].

***1.5.3 Metabolism of ApoB100-containing lipoproteins.*** ApoB100 is synthesized and expressed in the liver, consisting of 4,536 amino acids[78]. It's characterized by its large size, hydrophobic nature, and a structure composed of five domains: βα1, β1, α2, β2, and α3[78]. ApoB100 plays an integral role in the assembly of VLDL. In the ER, the microsomal triglyceride transfer protein (MTP) loads ApoB100 with triglycerides and cholesterol esters. ApoB100 undergoes maturation in the Golgi, where additional triglycerides are loaded[79]. The availability of triglycerides in hepatocytes directly impacts VLDL assembly, leading to the degradation of about 50–80% of ApoB100 in hepatocytes before the formation of nascent VLDL[79]. The initial VLDL is secreted and interacts with HDL, acquiring apoE, apoCII, and cholesterol esters in exchange for triglycerides through the CETP[72]. This process results in the formation of mature VLDL, which transports triglycerides from the liver to peripheral tissues. Initially, apoE can be recognized on remnant VLDLs by hepatic LDLR and also LDLR-related protein 1 (LRP-1), but as VLDLs remain in circulation and lose more triglycerides, they are eventually converted to cholesterol-rich LDL, exposing the ApoB100 binding site of the LDLR[54]. Additionally, PCSK9 can bind to LDL and IDL but not to VLDL, suggesting that hydrolysis during the VLDL-to-LDL transition also reveals the ApoB100 binding site of PCSK9 (**Fig. 6**)[80]. ApoB100-containing lipoproteins bind to proteoglycans near cell surface receptors, such as HSPG[56]. However, ApoB100 can also bind to proteoglycans in the arterial wall, leading to the retention of LDL and contributing to the development of atherogenic plaque[73].

Furthermore, each LDL particle contains a single copy of ApoB100, suggesting ApoB100's potential use as a direct atherogenic marker[72].

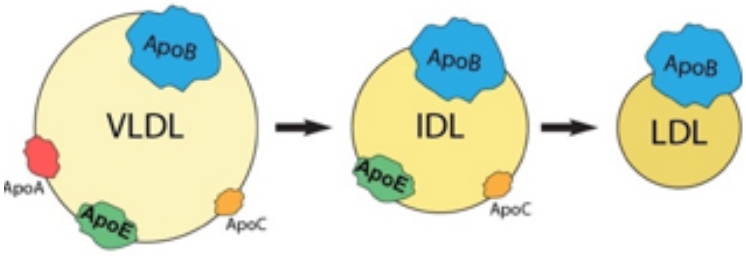


**Figure 6: Demonstrates the transition from VLDL to LDL.** As VLDL circulates, they lose triglycerides through hydrolysis leading to the formation of IDL and LDL revealing LDLR's apoB100 binding site[54].

***1.5.4 ApoB editing.*** Apolipoprotein B is present in two forms: apoB100 and apoB48. In humans, ApoB100 is found on VLDL, IDL, and LDL, while apoB48 is present on chylomicrons. ApoB100 has a molecular mass of 540000 Da and is composed of 4536 amino acids, whereas apoB48 constitutes 48% of the mass of apoB and is composed of 2512 amino acids[81]. ApoB48 is formed in enterocytes where post-transcriptional RNA editing results in a premature stop codon through the action of Apobec-1[82]. Notably, Apobec-1 is expressed exclusively in the small intestine of humans and most mammals; however, it is absent in the liver[83]. Importantly, mice do express Apobec-1 in the liver, with ~70% of liver-derived ApoB being ApoB48[84]. Therefore, studies of

lipoprotein metabolism in experimental mice need to consider this. While apoB100 binds the LDLR, ApoB48 does not since it's missing the site that is responsible for binding[85]. Similarly to ApoB100 in the liver, ApoB48 in enterocytes are synthesized in the ER, where the MTP loads it with triglycerides, phospholipids, and cholesterol esters, forming the pre-chylomicron[82]. The pre-chylomicron is transported to the Golgi, where apolipoproteins are incorporated, such as ApoAI, leading to its exit from enterocytes[86].

***1.5.5 LDL.*** LDL is the primary carrier of cholesterol; it transports around 67% of cholesterol to peripheral tissues such as the adrenal glands[87]. LDL has a density of 1.019 to 1.063 g/ml, and LDL particle size can vary from 20 to 25 nm[87]. LDL consists of an internal core made primarily of cholesterol esters, some triglycerides, and free, unesterified cholesterol[71]. The lipid core is surrounded by a phospholipid layer with a single copy of ApoB100 on the cell surface. ApoB100 is the exclusive apolipoprotein on the surface of LDL[71]. All tissues receiving LDL express the LDLR on their membranes, which is capable of recognizing ApoB100[88]. The LDL not internalized by peripheral tissues is returned to the liver[64]. LDL particles are mainly formed within the circulation from precursors (VLDL) secreted by the liver and IDL[64]. As VLDLs circulate, they lose triglycerides through hydrolysis by lipases (lipoprotein lipase or hepatic lipase) and gain cholesterol esters through lipid exchange reactions, converting to the short-lived (IDL) and finally to cholesterol-rich LDL[73 89]. LDL's role is to transport cholesterol from the liver to the peripheral organs, but the high concentration of cholesterol makes LDL a key contributor to cardiovascular disease.

***1.5.6 PCSK9-LDL binding.*** PCSK9 binds to LDL through a protein-protein interaction with ApoB100[90]. There are differing views on how LDL binding affects PCSK9 activity. Some studies suggest that LDL inhibits PCSK9's ability to bind to the LDLR, reducing receptor degradation[54]. Others believe LDL binding protects PCSK9 from furin-mediated proteolysis, preserving its ability to bind the LDLR[87].

In humans, LDL production and clearance are balanced. LDLR clears not only LDL but also VLDL remnants that have acquired ApoE, an LDLR ligand. PCSK9 can bind to IDL and LDL but not to VLDL, suggesting that the remodelling of VLDL into IDL and LDL exposes the PCSK9 binding site on LDL-ApoB100[54]. The secretion of PCSK9 and VLDL from the liver may increase the plasma presence of ApoE-containing VLDL and chylomicron remnants by limiting their hepatic clearance via the LDLR[80]. This enhances lipid transport to peripheral tissues, which indicates PCSK9's role during nutrient limitation[54]. In this model (**Figure 7**), with VLDL levels being high relative to LDL in circulation, there would be less PCSK9 bound to lipoproteins resulting in more PCSK9 available to bind and mediate the degradation of LDLR[91]. As the VLDLs remodel into IDL and LDL, PCSK9 increasingly binds lipoproteins rendering it inactive[54]. Thus, this process of negative feedback control on PCSK9 activity through its ability to bind LDL would eventually lead to increased clearance of lipoproteins through the LDLR[92]. Therefore, when food is scarce, having more circulating triglycerides could be advantageous, as it maximizes the dispersion of energy-rich fatty acids to peripheral tissues before they are cleared[92]. However, in a diet rich in fat and cholesterol, this role could lead to increased LDL-C levels and a higher risk of cardiovascular disease[90].

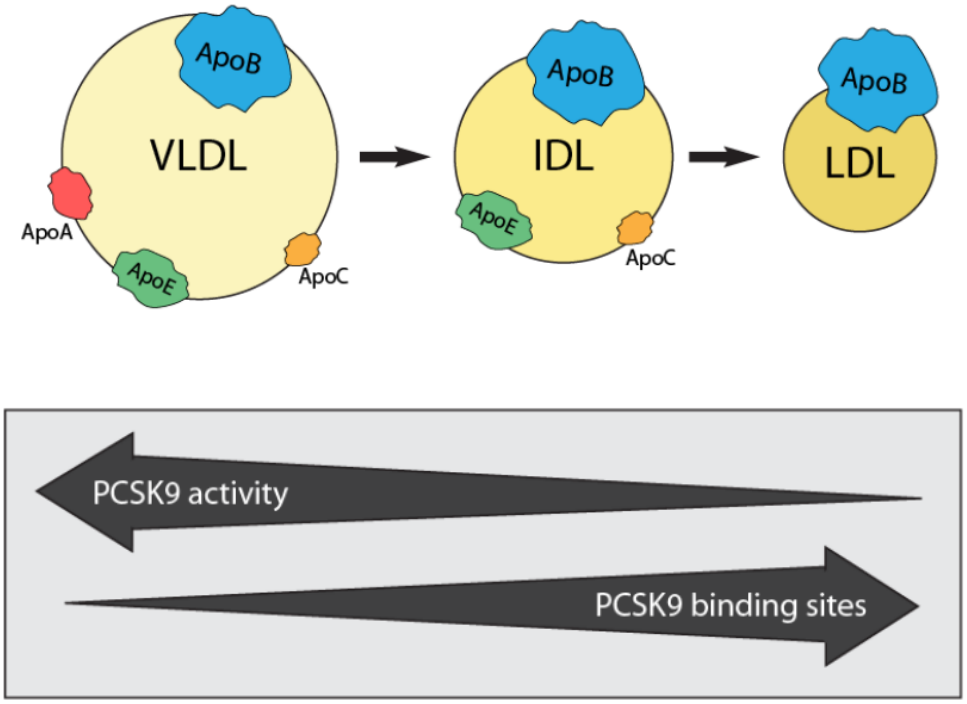


**Figure 7: Representation of PCSK9's role during nutrient limitation.** As are more VLDLs in circulation, less PCSK9 is bound to lipoproteins suggesting that more unbound PCSK9 is available to bind the LDLR, leading to lysosomal degradation. Seeing that VLDL loses triglycerides in circulation through hydrolysis by lipases forming IDL and LDL, exposing the apoB100 binding site, this allows PCSK9 to bind the lipoproteins. Since more PCSK9 is bound to lipoproteins, less PCSK9 is available to bind the LDLR, causing more LDLR present on the cell surface available to clear lipoproteins from the circulation[54].

Approximately 30–40% of PCSK9 in human circulation is bound to LDL[90]. This binding affects the amount of free PCSK9 that can bind to the LDLR[93]. While LDL inhibits PCSK9's ability to bind to cell surface LDLR, it does not sterically interfere with PCSK9's binding to the EGF-A domain. PCSK9 can bind simultaneously to LDL and the LDLR, as the binding sites for each are

in different regions of PCSK9[87]. Instead, LDL may act as a negative allosteric effector of LDLR binding in the catalytic domain of PCSK9, perhaps by stabilizing a native autoinhibitory conformation of PCSK9[41]. If so, when bound to LDL, PCSK9 would have a reduced affinity for LDLR[90]. Furthermore, studies suggest that HSPGs and LDL share a binding site in that, once PCSK9 is bound to HSPGs, LDL no longer can interfere with its binding to LDLR[56]. Understanding this mechanism could help identify a target for developing a small-molecule inhibitor[93].

Our lab has previously identified critical regions in PCSK9 involved in LDL binding, including the involvement of an N-terminal intrinsically disordered region (IDR) in the PCSK9 prodomain[1]. Interestingly, deletion analysis has identified this region as a negative allosteric regulator of PCSK9-LDLR binding[3]. This creates the possibility of discovering a target sequence to develop a molecule that could bind to the PCSK9 allosteric site in the prodomain and cause inhibition of LDLR binding, in effect mimicking the PCSK9-LDL interaction. The lab has also identified residues critical for LDL binding, specifically regions in the prodomain and the C-terminus[1]. The GOF S127R mutation in the prodomain of PCSK9 abolished LDL binding, as did the R496W mutation in the C-terminus[90]. These residues are positioned on the same molecular plane, suggesting LDL molecules interact with PCSK9 in two regions (**Fig. 8**)[1]. Our lab has tested numerous GOF mutations for effects on LDL binding, as observed in the figure below, and all the residues that abolish LDL binding are located on the same molecular plane[1].

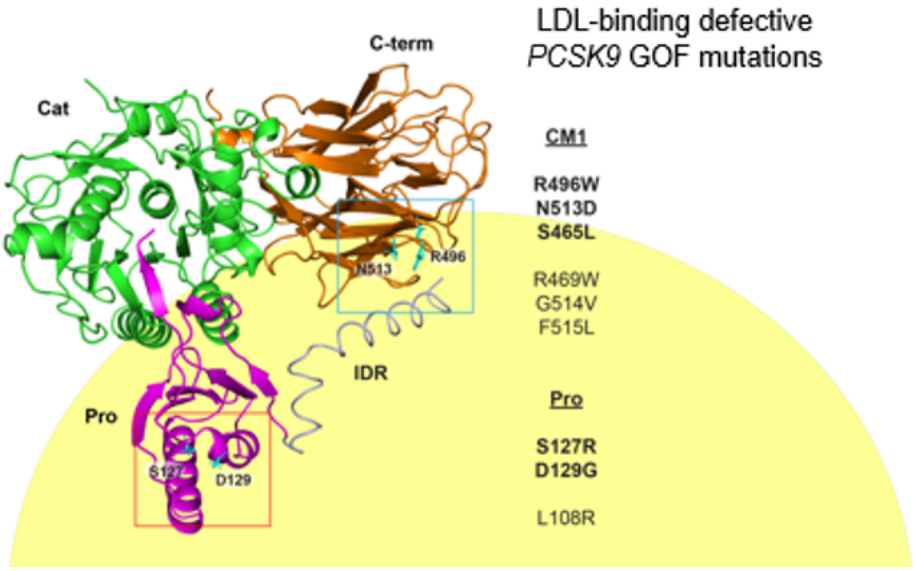


**Figure 8: Illustration of PCSK9 binding to LDL.** The GOF mutation in the PCSK9 prodomain and C-terminus domain that disrupts LDL binding are listed demonstrating that they are located on the same molecular plane. The yellow molecule represents an LDL molecule. This diagram was designed by **Sarkar et al, 2022.**

## 1.6 Study rationale and overview.

Since the discovery of PCSK9, several treatments targeting it have been developed to treat FH. However, there are many limitations with these treatments, thus requiring more knowledge to develop additional treatment strategies. As mentioned above, GOF mutations in PCSK9 notably result in FH; however, there remain many unknowns regarding how many of these mutations affect PCSK9's binding mechanisms to the LDLR and LDL[1]. Therefore, further examination of GOF mutations in PCSK9's prodomain is warranted to enhance understanding of the underlying mechanisms of action. Accordingly, our lab has identified critical residues involved in LDL binding[1]. Additionally, a variant of PCSK9 lacking 21 amino acids in the prodomain (aa 31-52),

termed del53-PCSK9, dramatically increases LDLR-dependant cell uptake, identifying this region as autoinhibitory[2]. This could suggest that certain residues in the prodomain could play a critical role in LDL and LDLR binding[90]. In addition, there is a helical region in PCSK9's prodomain located in proximity to the D129 residue which is responsible for binding to the HSPGs facilitating PCSK9s binding to the LDLR[56]. GOF mutations in this helical region have been associated with FH, however their mechanism of action remains unknown. Moreover, in between PCSK9 residue S127 and D129, is a highly conserved residue, G128. G128 residue has been identified in species producing Lp[a] (humans and old-world apes) but is an alternate amino acid in other species. Studies have shown that PCSK9i-mAbs reduce Lp[a] formation, suggesting that the G128 residue could be implicated in Lp[a] metabolism[75]. For this study, several residues in PCSK9 prodomain in these locations of interest were investigated for their role in LDL and LDLR binding to further define the PCSK9-LDL binding site and potentially enhance the understanding of PCSK9's structure and function in terms of its interaction with the LDLR. The study has three main focuses:

1- Further analysis of the regions in PCSK9s prodomain identified as important in LDL binding, with a specific focus on the D129 residue.
2- Observing the residues in the arginine-rich HSPG binding motif located in PCSK9's prodomain to understand its role in binding to LDL.
3- Studying a conserved residue in PCSK9 prodomain present in species known to produce Lp[a] to assess PCSK9's potential role in Lp[a] formation.

# Chapter 2: Structure-function analysis of regions in PCSK9 prodomain identified as important in LDL binding

## 2. 1 Introduction

Previous work identified that mutations in the S127 residue of PCSK9, including the S127R GOF mutation associated with FH, abolish LDL binding, thus demonstrating the importance of this residue in LDL binding[1]. As well, the D129G natural GOF mutation abolished PCSK9-LDL binding suggesting the introduction of a flexible glycine residue nearby S127 could affect its positioning[1]. D129 is located near the S127 residue, so this amino acid could potentially interact with S127 and interfere with its binding to ApoB100 or could be directly interacting with ApoB100[1]. **Figure 9A** shows this region in the crystal structure of PCSK9 (generated with PyMol software) and the predicted binding interactions of S127 and D129. D129 forms a side-chain hydrogen bond with Y107 and a main-chain interaction with S127. Another GOF mutation that is reported in a PCSK9 database associated with FH is D129N. As seen in **Figure 9B**, this mutation modelled *in silico* using PyMol shows an extra side-chain bonding interaction with S127. Therefore, there are two possibilities to be considered for the mechanism-of-action of D129 mutations: either 1) they prevent the binding interaction with Y107, or 2) they interfere with S127. Indeed, the S127 side-chain hydroxyl group could be binding to ApoB100[1]; however, if occupied by Asn at position 129 (as in the D129N mutation), this interaction would not occur. To further understand these mechanisms, D129 natural GOF mutations (D129G and D129N) a conservative mutation (D129E), or alanine substitution (D129A) were tested for effects on PCSK9's interactions with LDLR and LDL.

It has been previously shown that a truncated variant of PCSK9 lacking the N-terminal 21 amino acids in the prodomain (aa 31–52 following the signal sequence cleavage site), termed del53-PCSK9, displays dramatically increased LDLR binding affinity and LDLR-dependent cell uptake. This deletion affects the intrinsically disordered region (IDR) of the prodomain, which is positioned far from the catalytic domain which is responsible for the binding to the EGFA domain of the LDLR, thus indicating an allosteric autoinhibitory effect on PCSK9's ability to bind the LDLR[94]. The Lagace lab has also shown that the IDR is involved in LDL binding via the formation of an amphipathic helix that aligns an interdomain interaction with the C-terminal domain[3]. Taken together, the current information indicates an important role of the prodomain in PCSK9's binding interaction with LDL, either as a direct binding target of LDL-apoB100 or through an allosteric conformational effect. Since the IDR regulates both LDL and LDLR binding by PCSK9, this suggests an interrelationship between LDL binding and autoinhibition of LDLR binding by the prodomain IDR. In this Chapter, we looked further at the role of the key D129 residue on PCSK9's binding interactions with LDL and the LDLR.

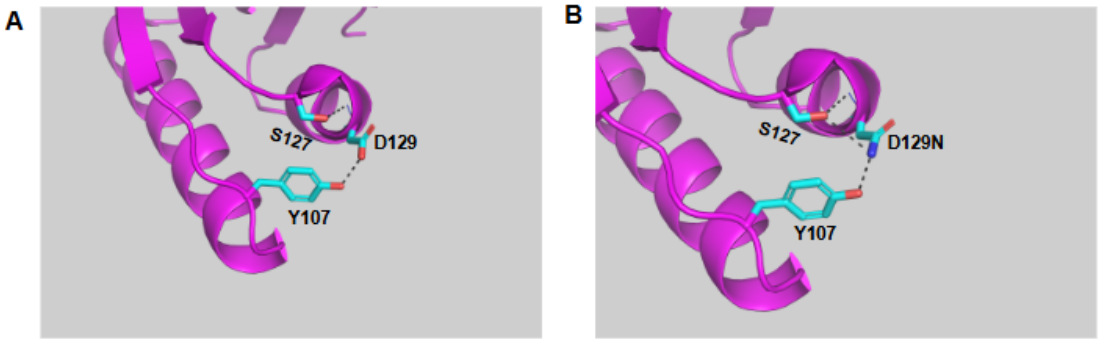


**Figure 9: Recreation of PCSK9 prodomain using pymol software demonstrating interactions within. A)** PCSK9 protein structure demonstrating D129 main chain interaction with S127 and side chain interaction with Y107. **B)** PCSK9 protein structure showing the GOF mutation D129N

predicted interactions with S127 and Y107, demonstrating a second side chain interaction with S127.

## 2.2 Results

**PCSK9 mutations in the prodomain do not affect autocatalytic processing and secretion**

The D129 residue is highly conserved among species and mutations such as D129G have been identified as causative for FH, but its GOF mechanism of action remains unknown[1]. Therefore, to assess the importance of this amino acid for LDLR and LDL binding, the production, expression, and secretion of these various amino acid substitutions at the D129 position were tested. These were D129G and D129N, both being FH-associated GOF mutations, along the D129E (conservative substitution) and D129A. We also tested Y107F to disrupt an intramolecular bond between D129 and Y017. For these experiments, HEK293 cells were transiently transfected with equal amounts of the various D129 mutant constructs or wild-type (WT)-PCSK9, and the whole cell extract (WCE) was harvested. Actin (loading control), precursor PCSK9, and mature PCSK9 were detected by western blot. The detected band at ~72 kDa represents precursor PCSK9 prior to prodomain cleavage, showing roughly equal production and expression of the mutants compared to WT-PCSK9 (**Fig. 10A**). However, there is a decrease in production of mature PCSK9 (~60kDa) for all the D129 mutants tested as well as Y107F, suggesting these mutations may impact the auto-cleavage process. The conditioned medium was also collected from the transiently transfected HEK293 cells, and an immunoprecipitation was performed. PCSK9 is produced in the cells, and the mature cleaved form is secreted into circulation. Compared to WT, three of the D129 mutants (D129G, D129A, and D129N) exhibited lower secretion levels, whereas the D129E and Y107F mutants appeared to be secreted equally to WT (**Fig. 10B**).

**D129 residue plays a role in cell surface LDLR binding**

As a preliminary test for effects on LDLR binding affinity, all D129 mutants were tested for cell uptake in LDLR-overexpressing HEK293 cells. This convenient assay allows for rapid screening of mutant forms of PCSK9 since HEK293 cells which express low levels of endogenous LDLR and so do not internalize appreciable amounts of PCSK9 added to the culture medium unless the LDLR is overexpressed. An LDLR-expressing plasmid was transiently transfected into HEK293 cells, while others received the empty vector as a control for any non-LDLR-related cell association. WT-PCSK9 or variants (D129 mutants or Y107F) present in the conditioned medium were then incubated with the cells at a physiological concentration of 3 μg/mL for 2 h in the presence of 100 μM chloroquine to prevent lysosomal degradation of the internalized PCSK9. The cells were harvested, and a western blot was performed using the WCE. The top panel in **Figure 10 C** shows the LDLR expression levels, showing that in the vector-transfected control cells, there is no LDLR detected. The PCSK9 band in the western blot represents the PCSK9 that bound to LDLR, was internalized and accumulated in the cells. Quantification of blots from 2 independent experiments provides evidence that mutations in D129 increased LDLR-dependent cell uptake of PCSK9 to various degrees, whereas there was no effect of the Y107F mutation. This includes the D129A mutation, which would not be involved in a side-chain interaction. This suggests that the observed increased LDLR binding is a function of the lack of an aspartate at this site, rather than the gain of another amino acid side-chain interaction.

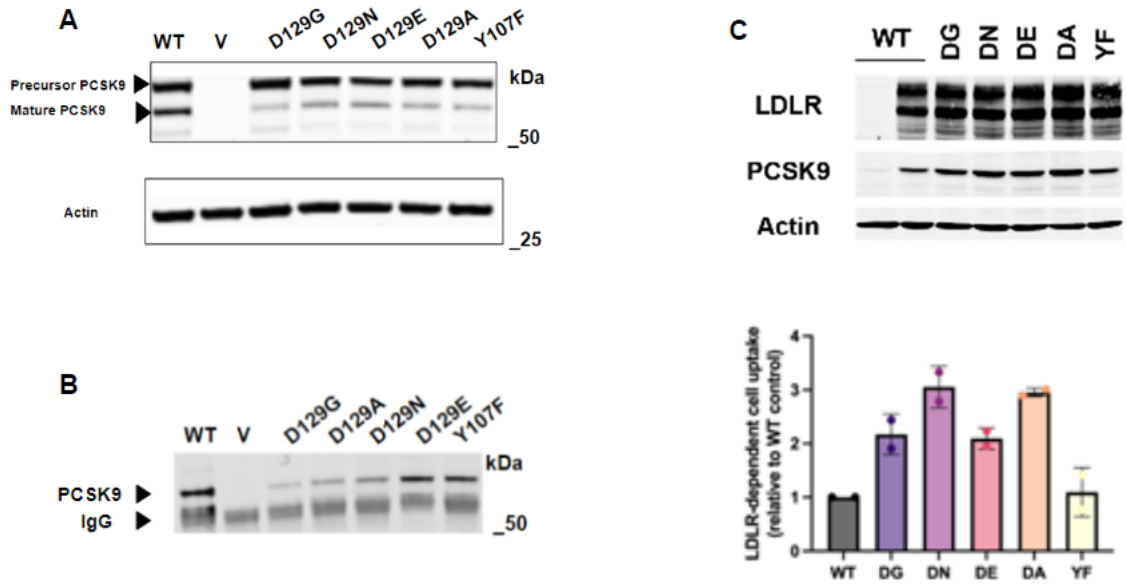


**Figure 10: D129 seems to play a role in LDLR degradation. (A)** PCSK9 mutants express and produce similarly to wild type. Following the transient transfection of HEK293 cells, the whole cell extract was harvested. The expression of transient PCSK9 was determined by western blot. The full-length PCSK9 and mature PCSK9 are shown (n=3). **(B)** PCSK9 mutant's overall processing and secretion appear delayed. Following transient transfection of HEK293 cells, the medium was conditioned for 48 hours. The medium was concentrated, an immunoprecipitation and a Western blot were performed to visualize the amounts of PCSK9 (n=3). **(C)** Cell uptake was tested in the LDLR-transfected HEK293 cells for the D129 and Y107 mutants. Following a 2 h incubation with 3µg/mL in the presence of 100µM chloroquine (top). The LDLRs were isolated and quantified by Western blot using actin (bottom). Shown are the representative experiments (n=2).

We also introduced the D129A mutation into del53-PCSK9 and tested for effects on LDLR uptake to determine if the mutation was acting on the same mechanism to increase LDLR binding.

Unfortunately, in these experiments results with the single D129A mutation did not correlate with previous results (**Fig. 11A**). Although the LDLR-dependent uptake assay in HEK293 cells is a good method for initial characterizations, it does tend towards inconsistencies. To perform a more detailed analysis of the D129A mutation, we next proceeded to purify this PCSK9 variant. A stable cell transfection with FLAG-tagged WT and D129A versions of PCSK9 was conducted to create large amounts of both to be used directly in LDLR binding studies (**Fig. 11B**). HEK293S suspension cells produce small amounts of endogenous PCSK9, which makes these cells ideal to use as a control. WT-PCSK9 and D129A mutants were successfully purified in large amounts using a combination of FLAG-affinity and size-exclusion chromatography steps. In addition, a western blot was performed confirming the purity of WT-PCSK9 and D129A produced. In **Figure 11C**, the band located around 60kDa represents the mature secreted PCSK9 Cat/C-term domain fragment. In addition, the gel was stained with Coomassie blue to confirm the purity of the protein. As seen in **Figure 11D**, we observed a band at ~60kDa corresponding to the larger Cat/C-term domain fragment and a band at ~16 kDa corresponding to the associated prodomain confirming the purification of PCSK9 and the lack of contaminants.

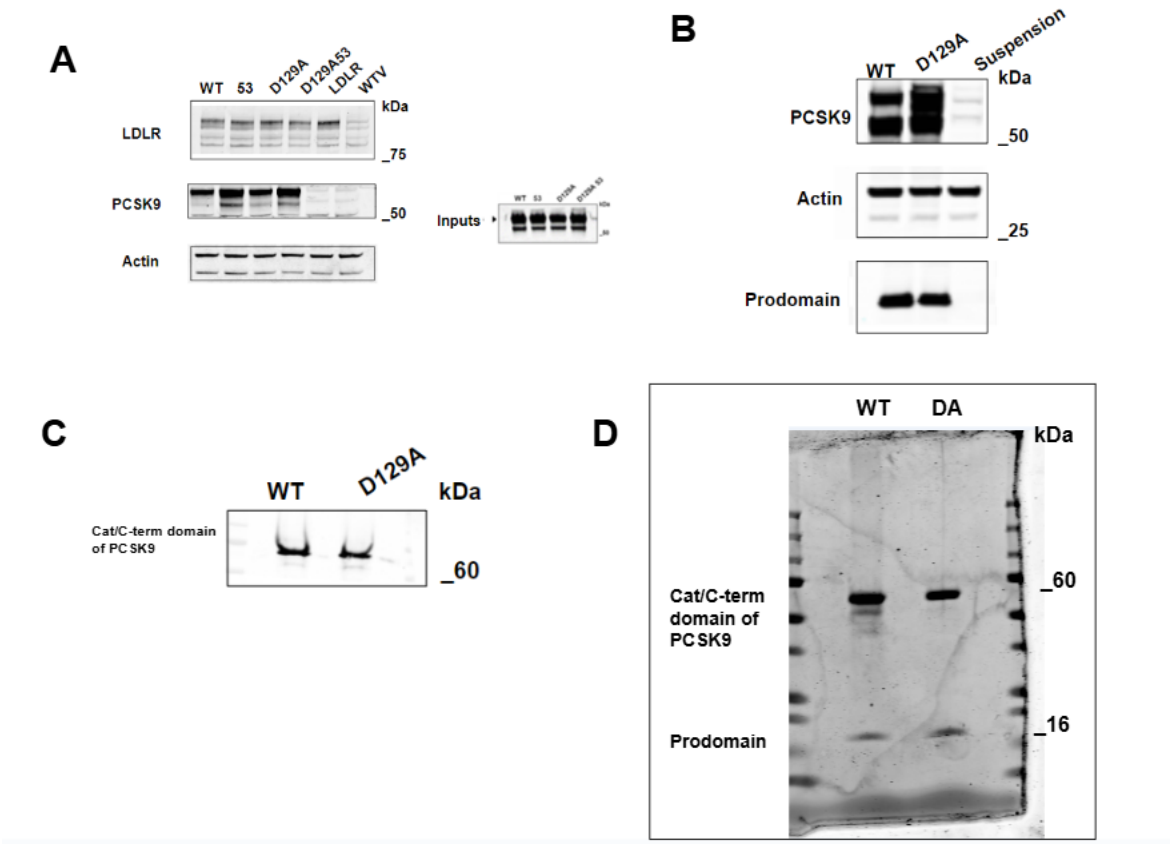


**Figure 11. The D129A LDLR-dependant cell uptake values differed from previous experiments. (A)** LDLR dependant-cell uptake was tested in LDLR-transfected HEK293 cells for WT, D129A, del53-PCSK9, and D129A-del53-PCSK9 mutants. Following a 2h incubation with 3 µg/mL of the mutants in the presence of 100M chloroquine. Shown are the representative experiments (n=3). **(B)** Stable cell line production of WT and D129A. HEK293s (suspension cells) were transiently transfected with purified D129A and WT. The whole cell extract was harvested and the expression of the different PCSK9 was determined by a western blot. **(C)** Following the purification of WT and D129A-PCSK9, the purified proteins were run on a western blot to determine their purification (n=1). **(D)** The gel was stained with Coomassie blue.

In a plate assay format, equal amounts of purified WT, D129A, and delta-53 were incubated with immobilized extracellular domain (ECD) of LDLR to test its binding. Following washes, the plate

was incubated with a biotin-labeled antibody to PCSK9 followed by streptavidin-HRP and ELISA substrate to generate a chromophore for detection. The absorbance results at 450 nm were then observed using a Synergy plate reader. As seen in **Figure 12A**, the D129A had a significant increase in LDLR binding compared to WT-PCSK9, but the increased binding was lower than that of del53-PCSK9. These results confirm that the D129A mutation increases LDLR binding, identifying it as a GOF mutation. In addition, to further confirm the effects of D129A on LDLR, an LDLR degradation assay was performed using WT-PCSK9 and D129A-PCSK9 added to the culture medium of Hepa1c1c7 cells. Different concentrations of WT-PCSK9 and D129A-PCSK9, starting at 1.5 µg, 2.5 µg, and 5 µg, were added to the cells. As seen in **Figure 12B**, D129A increases LDLR degradation compared to WT-PCSK9. This confirms that D129A increases LDLR binding and degradation, further demonstrating it's a GOF mutation. As well, confirms the D129 residue is important for LDLR binding.


**Figure 12. D129A increases LDLR binding and LDLR degradation. (A)** A plate assay was performed with equal amounts of purified WT, D129A, and del53-PCSK9 incubated with 10 µg/mL of the ECD of the LDLR. The plate was incubated with a biotin-labelled antibody,

streptavidin-HRP, and ELISA substrate to be observed using a synergy reader. Shown is a representative of the quantitative results from the synergy reader (n = 3). Significant changes in LDLR expression compared to WT-PCSK9 were determined by a one-sample t-test using GraphPad Prism 10: **p < 0.01 and ***p<0.001. **(B)** Hepa1c1c7 cells were cultured in a sterol-deficient medium, treated with equal amounts of WT and D129A-PCSK9, and incubated for 4h at 37ºC. After 4h, the WCE was harvested and run on a western blot. Shown is a representative experiment (n=3).

**D129 residue is important in LDL binding.**

The D129 mutants were also tested for LDL binding to further analyze their impact. To evaluate LDL binding, the concentrated conditioned medium was adjusted and incubated with equal amounts of PCSK9 alongside isolated human LDL. Using an Optiprep density gradient, LDL-bound, and unbound PCSK9 were separated by ultracentrifugation. Immunoprecipitation of PCSK9 followed by Western blot was performed to analyze the LDL-bound PCSK9, which showed that all D129 mutants abolished LDL binding (**Fig. 13A**). However, the Y107F mutation also showed a slight decrease. This experiment was repeated without the immunoprecipitation step, further revealing the decrease in LDL binding in the Y107F-PCSK9 (**Fig. 13B**). The quantification of WT-PCSK9 and Y107F-PCSK9 LDL binding indicated a significant decrease in LDL binding in Y107F compared to WT. This demonstrates the importance of the D129 mutation in LDL binding and the role of the Y107-D129 interaction.

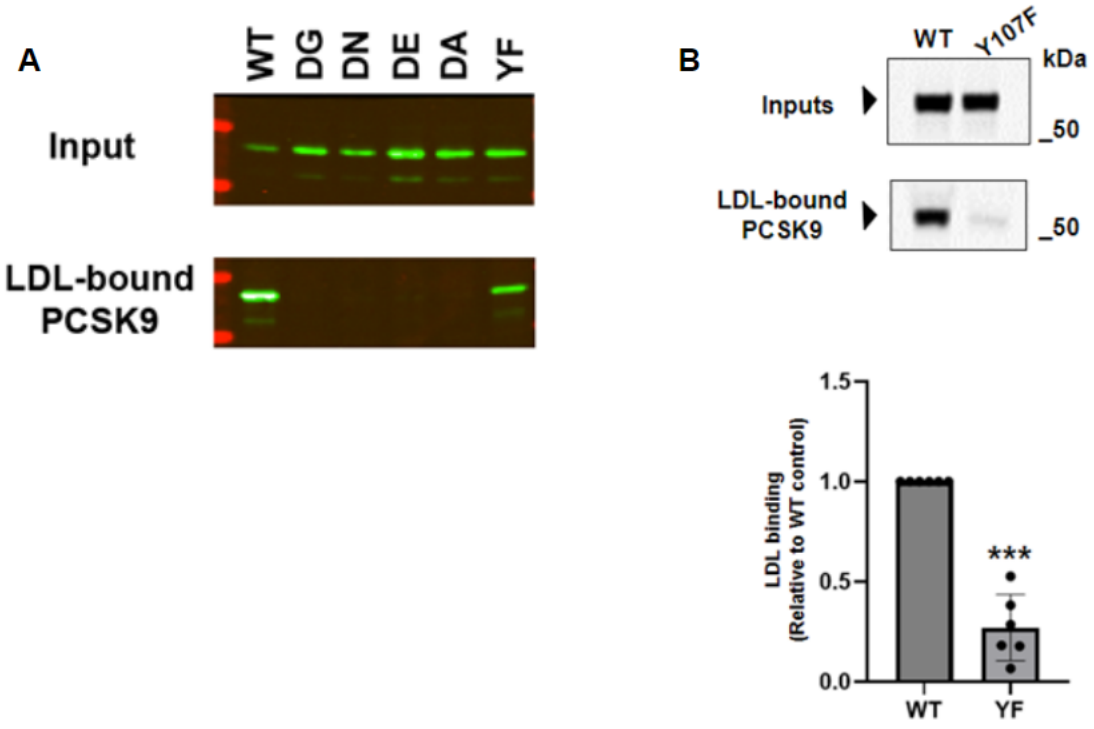


**Figure 13. D129 residue is important in LDL binding and D129-Y107 interaction seems to play a role in LDL binding. (A)** D129 is critical for LDL binding. After the transient transfection of HEK293 cells, the PCSK9 conditioned medium was collected and concentrated. The conditioned medium was adjusted for equal amounts of PCSK9 and incubated with LDL. The optiprep density gradient separated the LDL-bound and unbound PCSK9, the unbound was found at the bottom of the tube. After ultracentrifugation, the LDL fraction was removed. The PCSK9 from the LDL fraction was determined by immunoprecipitation and followed by Western blotting. **(B)** Y107 is important for LDL binding. After transient transfection of HEK293 cells, the PCSK9 conditioned medium was collected and concentrated. The conditioned medium was adjusted for equal amounts of PCSK9 and incubated with LDL. The optiprep density gradient separated the LDL-bound and unbound PCSK9, the unbound was found at the bottom of the tube. After ultracentrifugation, the LDL fraction was removed. The PCSK9 from the LDL fraction was

determined by immunoprecipitation and followed by Western blotting (top). The results from the western blots were quantified using WT and shown as a representation (n=3). Significant changes in LDL binding compared to WT-PCSK9 were determined by a one-sample t-test using GraphPad Prism 10: ***p<0.001.

## 2.3 Discussion

Two of the D129 mutations that we tested are naturally occurring FH-associated GOF mutations (D129N and D129G) while two were novel mutations. For all these mutants, the self-processing of PCSK9 to its mature form was lessened compared to that of WT-PCSK9 (**Fig. 10A**). This suggests that the D129 mutations may interfere with the autocleavage process since all samples contained equal amounts of the precursor PCSK9. Thus, particular interactions of the natural D129 residue could be important for PCSK9 maturation. It is possible that delayed processing of the D129G and D129N mutants in humans could lead to a GOF mechanism, such as an increased effect on the secretion of apoB100 in the form of VLDL, as has been suggested for the S127R mutation which also exhibits delayed self-proteolysis and maturation[95]. However, while processing and secretion appeared to be somewhat delayed for the D129 mutants tested, they nevertheless were all secreted (**Fig. 10B**). Thus, the identified FH-associated GOF mutations affecting D129 (D129G and D129N) could be acting within the extracellular pathway of LDLR degradation and/or on the PCSK9-LDL interaction. Therefore, we proceeded to test these mutant PCSK9 proteins in LDLR and LDL binding assays.

We found that all substitutions tested for D129 increased LDLR-dependent cell uptake of PCSK9 (**Fig. 10C**). This included D129A, which would not be involved in the side-chain interaction since the alanine is non-reactive. These findings suggest that D129 participates in intramolecular

interactions that lower PCSK9-LDLR binding affinity, so this residue is autoinhibitory. A truncated version of PCSK9 lacking the N-terminal 21 amino acids, termed del53-PCSK9, displays dramatically increased LDLR binding affinity, indicating that the N-terminal IDR is also involved in autoinhibition[3] above. Since this region could bind in the proximity of the D129 residue, this suggests that they could be acting through the same mechanism[23]. Therefore, the D129A mutant was introduced into the del53-PCSK9-expressing plasmid to test if the effects of LDLR-dependent cell uptake are redundant (acting on the same mechanism) or additive (acting on a different mechanism). LDLR-dependent cell uptake experiments were conducted; however, the results were inconclusive. As seen in **Figure 11A**, the D129A mutant construct uptake into cells was at lower levels than seen before, and we were unable to recapitulate the previous increase in LDLR-dependent cell uptake. The reasons for this discrepancy are unknown but could involve changes in post-translational modifications of the secreted PCSK9 during cell culture or otherwise changes to the D129A mutant protein. While the LDLR-dependent cell uptake assay is a rapid and convenient method for additional screening, it can yield variable results, necessitating other techniques to more definitively determine the effects of mutations on PCSK9's ability to bind LDLR. Therefore, we opted to conduct LDLR binding assays using purified D129A-PCSK9 as opposed to using the conditioned medium to determine if the D129A does indeed increase LDLR binding. The WT and D129A-PCSK9 proteins were purified using a stable cell line (HEK293s) (**Fig. 11B**). HEK293s cells grow in suspension providing large amounts of cells which in turn allows the production of a large amount of secreted recombinant PCSK9. WT-PCSK9 and D129A mutant were successfully purified, and an in vitro plate assay confirmed that D129A increases LDLR binding affinity compared to WT-PCSK9 by ~2.5-fold (**Fig. 12A**); however, this increased binding affinity was not to the same extent as that of del53-PCSK9. This suggests that the D129 residue in the

prodomain forms an interaction that allosterically lowers LDLR binding affinity under normal circumstances, resulting in autoinhibition. It remains to be determined whether the mechanisms of autoinhibition involving D129 and the IDR are partially overlapping. In future studies, the double mutant del53/D129A will be purified for use in comparative LDLR binding assays. Given the proximity of the D129 residue to the prodomain IDR and the fact that both the D129A mutation and deletion of the N-terminal 21 amino acids increase LDLR binding, we hypothesize that they are acting on the same mechanism, having redundant effects. Since the LDLR binding affinity is much greater for del53-PCSK9 than for D129A-PCSK9, this suggests that the autoinhibitory effect of the N-terminal IDR is mediated only partially through the D129 residue.

We also found that D129A-PCSK9 was more active than WT-PCSK9 in mediating cell surface LDLR degradation when added to the culture medium of mouse Hepa1c1c7 cells. Since this dose-dependent increase in LDLR degradation was ~2-fold (**Fig 12B**), similar to the observed increase for *in vitro* LDLR binding, this suggests the effect is due to increased binding affinity to LDLR, and not to another mechanism, such as increased binding to the beta-propeller of LDLR leading to improved downstream degradation in the endocytic pathway. Abnormal degradation of LDLR is associated with various health diseases, most notably FH. Therefore, D129 mutations that relieve its autoinhibitory effect, perhaps through disrupting its intramolecular contacts, would be expected to increase the binding of the mutant PCSK9 to the LDLRs on the surface of liver hepatocytes leading to increased LDLR degradation. Thus, our results provide insight into the D129G and D129N mutations that have been identified in FH patients[14], providing evidence that it is the loss of the D129 amino acid, and not the presence of glycine (D129G) or asparagine (D129N), that leads to hypercholesterolemia.

Through the introduction of various point mutations, critical regions in PCSK9 involved in LDL binding have been identified. These include the GOF mutation R496W mutation located in the C-terminus which abolishes LDL binding but does not impact PCSK9-LDLR binding[1]. In addition, it was found that GOF mutations S127R and D129G in the prodomain also abolished LDL binding[1]. These mutations are located in different regions of PCSK9; however, they are found on the same molecular plane. Many GOF mutations located on the same plane in the C-terminal domain have also shown a reduction in LDL binding[1]. Since LDL is a large particle, it could bind to PCSK9 in two regions, causing conformational changes. Alternatively, these two regions could act cooperatively to facilitate LDL binding to a single region of PCSK9, either the prodomain or the C-terminal domain. We found that all amino acid substitutions tested in D129 abolished LDL binding, including D129A (**Fig. 13A**) which was also found in a previous study in our lab regarding the S127 residue[1]. Thus, the adjacent S127 and D129 residues may form direct contacts with LDL-apoB100 that cannot be substituted by other amino acids at these positions, as even the conservative D129E mutation abolished LDL binding. When mutant forms of PCSK9, such as the D129 mutants, do not bind LDL there is more PCSK9 present in circulation that is active to increase degradation of the LDLR. We found that a Y107F mutation to prevent an intramolecular interaction between Y107 and D129, as seen in X-ray crystal structures of PCSK9 (**Fig. 9A**), decreased LDL binding compared to WT-PCSK9, but not as dramatically as the D129 mutations (**Fig. 13B**). During these studies, we determined that the immunoprecipitation protocol was not quantitatively capturing all the PCSK9 in the LDL fractions. Thus, unless there was an abolishment of LDL binding (e.g. D129G), LDL binding deficiencies were being masked. Thus, by direct western analysis of PCSK9 in LDL-containing fractions following Optiprep density gradient separation, we further observed a significant difference between Y107F-PCSK9 and WT-PCSK9.

These results suggest that the Y107-D129 bond is important for LDL binding; however, not necessary considering the Y107F mutation did not abolish LDL binding. Through its interaction with D129, Y107 might help maintain a specific conformation of the D129 and S127 residues, allowing optimal LDL binding. Importantly, if the apoB100 protein component of LDL binds the PCSK9 prodomain near this site, it could mimic the IDR autoinhibitory effect. Thus, mutations affecting known intramolecular bonds near the D129 site could affect both LDL and LDLR binding, as was seen for the D129A mutation.

# Chapter 3. The influence of heparan sulfate proteoglycans and arginine mutations on LDL binding

## 3.1 Introduction

Previous work has shown that PCSK9 binding to the LDLR is assisted by heparan sulfate proteoglycans (HSPG) acting as coreceptors on hepatocytes[4]. The HSPGs capture PCSK9, allowing optimal conditions for the formation of the PCSK9-LDLR complex (**Fig. 14A**). The LDLR-PCSK9 binding constant ($K_d$) has been estimated to be between 170–628 nm[56]. However, under normal physiological conditions, the plasma PCSK9 concentration is ~6-20 nm, indicating an unlikeliness that circulating PCSK9 would bind sufficiently to affect cell surface LDLR levels[56]. In addition, previous studies have shown that the LDLR has a higher binding affinity for LDL compared to PCSK9, suggesting that circulating PCSK9 would be less likely to impact LDL clearance via the LDLR[56]. This hints at the implication that other factors are necessary to facilitate the interaction between the LDLR and PCSK9, aligning with the idea that HSPG binding provides a localized concentration of PCSK9 at the hepatocyte cell surface[4]. There is a helical region in the prodomain encompassing residues 87–108 that includes five arginine residues, specifically R93, R96, R97, R104, and R105 that were identified as the binding site of HSPGs (**Fig. 14B**)[56]. Interestingly, it was found that the introduction of the S127R GOF mutation increased LDLR binding as well as HSPG binding. Given the fact that S127 is located near the HSPG arginine-rich loop motif, and the mutation introduces an arginine, this could increase PCSK9 affinity for the negatively charged HSPGs[4]. In this same study, it was also found that binding to HSPGs nullified the inhibitory effect of LDL on PCSK9-LDLR binding[4]. Thus, the arginine-rich helical region could play a role in LDL binding, or its binding to HSPGs could in some manner physically block LDL-apoB100 binding to the adjacent S127 and D129 residues[4].

There are several GOF mutations in PCSK9 involving the arginine residues in the helical region, including R105W, R96L, and R96C. The R105 and R96 residues have both been identified as critical residues involved in the interaction with the sulfate groups of HSPGs, although this has been identified as a cumulative effect, without any single residue being essential[56]. There are contradictory studies implying that the R105W and R96L are LOF mutations due to reduced autocatalytic processing, yet both mutations have been identified in Chinese patients exhibiting FH[96]. Our lab previously tested the R96L and R96C mutations for effects on LDL binding and noticed that the LDL-bound levels were similar to WT[1]; however, these results were achieved following immunoprecipitation of LDL-bound fraction, which could have masked any deficiencies. Therefore, the LDL binding of these mutations was reevaluated, along with R105W, with direct detection of PCSK9 in LDL fractions by western blot to further observe the role of these arginine residues in LDL binding and determine the nature of these mutations.

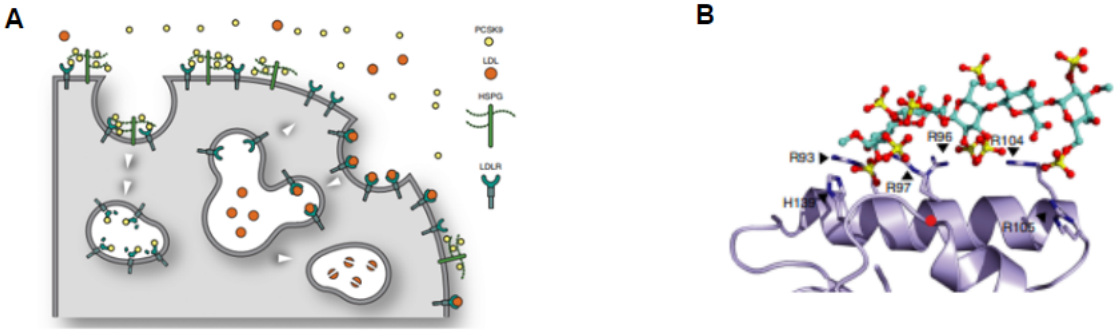


**Figure 14. Models further demonstrate the association between PCSK9 and HSPGs. (A)** Model representing the role of HSPG in PCSK9 on hepatocytes. This represents how the presence of HSPGs mediates the capture of PCSK9, presenting it to the LDLR and the complex is eventually internalized. As well, as the normal binding of LDL to the LDLR which does not require the

presence of HSPG. **(B)** Demonstrates the predicted binding surface of PCSK9 and HSPG showing key residues in PCSK9 required for binding. These models were used from **Gustafsen et al, 2017**[56].

## 3.2 Results

To analyze the effect of the mutations on PCSK9-LDL binding, equal amounts of PCSK9-R105W, PCSK9-R96L, and PCSK9-R96C containing conditioned medium were incubated with isolated human LDL. Finally, LDL-bound and unbound PCSK9 were separated using an optiprep density gradient via ultracentrifugation, as described above. A western blot was performed to analyze the LDL fraction PCSK9, and the results were quantified. This analysis confirmed our previous finding that the R96L variant maintained normal LDL binding, showing no significant decrease in LDL binding compared to WT-PCSK9. While we only performed 2 repeats for the R96C variant, it was clear from western blot data that this mutation also did not greatly affect LDL binding. However, the R105W mutation significantly decreased LDL binding compared to WT. These results suggest that the R105W GOF mutation acts by decreasing LDL binding, while R96 mutations do not (**Fig. 15**).

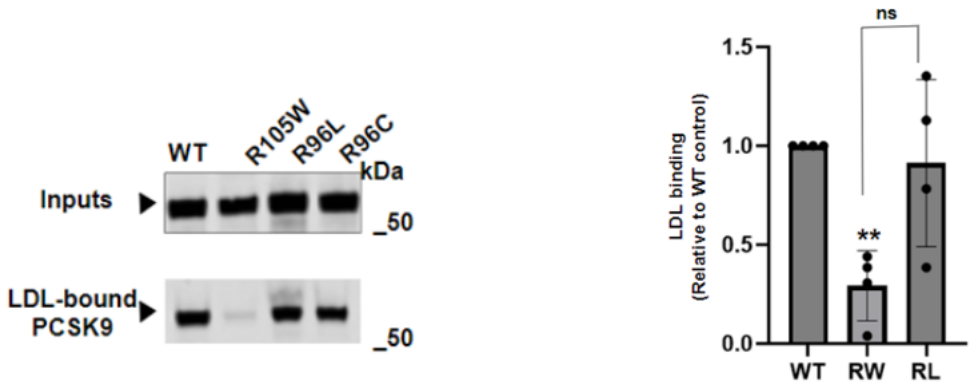


**Figure 15. R105 plays an important role in LDL binding (A)** R105 is important for LDL binding. After the transient transfection of HEK293 cells, the PCSK9 conditioned medium was collected and concentrated. The conditioned medium adjusted for equal amounts of PCSK9 was incubated with LDL. The Optiprep density gradient separated the LDL bound and unbound PCSK9, the unbound was found at the bottom of the tube. The LDL fraction was removed. The PCSK9 from the LDL fraction was determined and quantified by a Western blot (top). The results from the Western blots were compared to WT and shown as a representation (n=3). Significant changes in LDL binding compared to WT-PCSK9 were determined by a one-sample t-test using GraphPad Prism 10: **p<0.01.

## 3.3 Discussion

The GOF mutations R105W and R96L result in hypercholesterolemia and are situated in the arginine motif known to bind to HSPGs[4]. Our LDL binding analysis supports that the R105W GOF mutation may act, at least in part, through LDL binding, suggesting that the decreased LDL binding allows more circulating R105W-PCSK9 to bind to the LDLR, guiding it to lysosomal degradation. Even though the LDL binding is decreased in the R105W mutation, the HSPG binding requires

numerous arginine residues[4]. This cumulative effect on PCSK9-LDLR binding indicates that a single mutation would not considerably impact the overall effect. Furthermore, if R105W decreased HSPG binding (**Fig. 15**), this would be incompatible with a GOF mechanism since HSPG binding has been shown to facilitate the cell surface LDLR interaction in hepatocytes[56]. By contrast, the LDL binding result indicates that a singular mutation does have a significant impact on the binding and that the R105 residue plays a significant role in LDL binding. Since the R96L and R96C variants of PCSK9 maintained LDL binding, this suggests that these GOF mutations act through another mechanism.

The current data from the literature and our ongoing studies support that the arginine-rich helix together with the S127 and D129 residues constitute an important allosteric regulatory site in PCSK9. Deletion of residues 31–52 in PCSK9 (del53-PCSK9) dramatically improves LDLR binding[2], suggesting this deletion may not only relieve autoinhibition but also reveal the arginine motif to bind HSPGs, allowing increased LDLR binding[4]. In agreement, the Lagace lab recently collaborated with Dr. Derek Wilson's research group at York University to map potential intramolecular interacting sites of the N-terminal prodomain IDR using hydrogen-deuterium exchange mass spectrometry (HDX-MS). In this method, deuterium uptake in the PCSK9 occurs through rapid exchange with hydrogen atoms on exposed peptide backbone amides and the resulting changes can then be mapped using existing PCSK9 crystal structures. The access for HDX can be affected by protein conformational shifts and transient protein-protein interactions. This analysis showed that the highest increase in HDX for del53-PCSK9 compared to WT-PCSK9 occurred within the arginine-rich helical region of the PCSK9 prodomain (**Figure 16**), identifying this site as a potential interactor of the autoinhibitory IDR. As mentioned, this region is adjacent

to S127 and D129 and contains Y107 which, as investigated in Chapter 2, forms an intramolecular bond to D129. This finding supports the hypothesis suggesting that N-terminal IDR can recognize and bind to two regions in PCSK9: one in the prodomain (the arginine-rich loop) and the other in the C-terminus. In an aqueous environment, the IDR would bind within the prodomain, blocking the HSPG and LDL binding sites while causing autoinhibition of LDLR binding. If HSPGs at the hepatocyte surface can displace the IDR, this would relieve autoinhibition while also leading to a localized concentration effect on PCSK9 at the cell surface, thus facilitating LDLR binding/degradation. However, in a hydrophobic environment at the LDL surface, a conformation switch in the IDR to amphipathic helix formation would favour an electrostatic interaction with residues in the C-terminus. This by itself could relieve the autoinhibition, however, LDL-apoB100 binding to the allosteric site would maintain the inhibitory effect.

Since HSPGs and the autoinhibitory IDR possibly share a binding site, the R96L GOF mechanism could be causing a conformational change that may displace the IDR, possibly relieving the autoinhibition effect. Thus, future studies should involve the purification of R96 mutant forms of PCSK9 for a detailed analysis of its binding interaction with the LDLR to determine if there is increased binding to LDLR. Any decrease in IDR binding would relieve the autoinhibition, allowing PCSK9 to bind to the HSPGs and increasing PCSK9-mediated LDLR degradation.

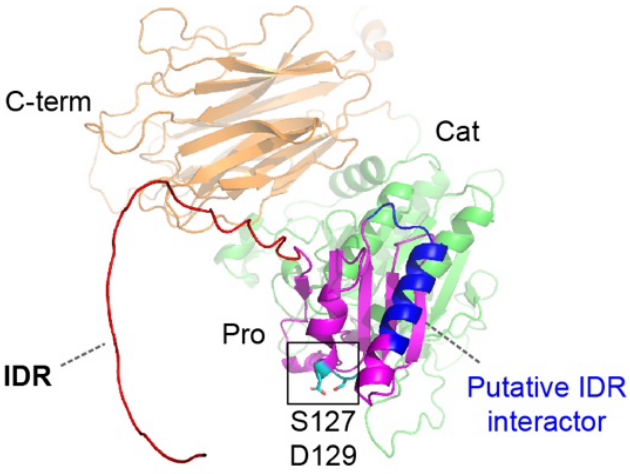


**Figure 16. The mapping of intramolecular interaction sites in PCSK9s N-terminal prodomain IDR using HDX-MS.** The site of the greatest increase in hydrogen-deuterium exchange for del53-PCSK9 compared to WT-PCSK9 is indicated in blue. This map reveals that the putative IDR interactor (blue) is located adjacent to S127 and D129 in the prodomain (purple) and the IDR (red) interacts with a specific region known as the arginine-rich helical region of the PCSK9 prodomain.

# Chapter 4: PCSK9 influence on Lipoprotein [a] production.

## 4.1 Introduction

Lp[a] has been discovered to play a role in cardiovascular disease, particularly atherosclerosis[97]. Lp[a] is a liver-derived lipoprotein that resembles low-density lipoprotein (LDL) but contains apolipoprotein B covalently bound to apo[a] through a disulfide bond. It is found in humans, non-human primates, and Old-World monkeys, but is absent in other mammals. Unlike LDL, which can be influenced by exercise and diet, Lp[a] levels are influenced by genetics[98]. While the physiological role of Lp[a] is not fully understood, some studies suggest it may be involved in wound healing by transporting cholesterol to the injury sites and facilitating the fibrinolysis process[99]. Nonetheless, it is known to have a role in cardiovascular disease.

Lp[a] is considered pro-atherogenic because it carries oxidized phospholipids. Inflammatory molecules within atherosclerotic plaques, such as foam cells, recognize Lp[a][100], which can lead to the deposition of cholesterol and oxidized phospholipids, further promoting plaque formation[99]. Recent research has shown that PCSK9 inhibitors, such as alirocumab, can reduce Lp[a] levels by 20–30%, whereas statins do not[76]. These studies demonstrated that PCSK9i-mAb therapy reduces Lp[a] formation but not its catabolism since neither PCSK9 nor alirocumab alters Lp[a] uptake[101]. Lp[a] binds poorly to the LDLR, and Lp[a] uptake rates remain similar in all FH patients, even those with homozygous FH (no LDLR present on the cell surface). In the presence of PCSK9, Lp[a] production by hepatocytes is increased, whereas it decreases in the presence of alirocumab[102]. Our lab previously researched an antibody that would bind to IDL and LDL (**Fig. 17A**), similarly to PCSK9 since it doesn't bind to VLDL[103]. This resulted in the identification of an antibody (4H11) that binds to the C-terminus segment of apoB100, blocking the interaction between PCSK9 and LDL (**Fig. 17B**). The C-terminus segment of apoB100 is responsible for one

of the apo[a] binding sites, which is critical in the formation of Lp[a] (**Fig. 17B**)[103]. This suggests that PCSK9 binding to LDL may facilitate the optimal positioning of LDL-apoB100, improving its interaction with apo[a] and increasing the production of Lp[a].

Noticeably, there is a poorly conserved amino acid located at position 128, located between S127 and D129. In humans, apes, and Old-World monkeys that produce Lp[a], a flexible Gly residue is present in the position (G128); however, it is not present in new world monkeys (G128R) or mice (G128S). The presence of Lp[a] in species with the G128 residue and the fact that PCSK9 inhibitors lower plasma Lp[a] levels suggest that substitution at this position could affect PCSK9-LDL binding affinity. If so, this could potentially be related to Lp[a] levels.

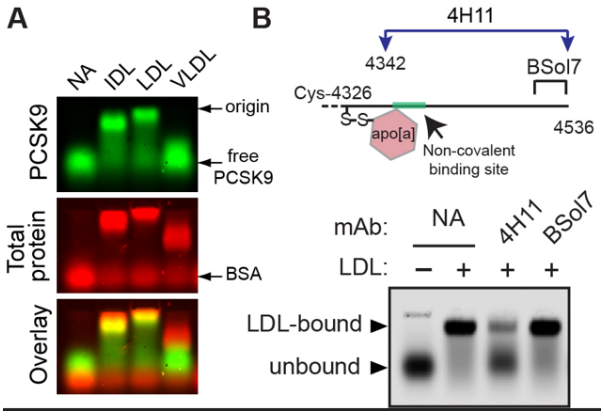


**Figure 17. The use of 4H11 antibody was investigated for its effects on PCSK9 binding. (A)** The results show that PCSK9 can bind IDL and LDL, but not VLDL. **(B)** Shows the C-terminus region of apoB, where the apoA binding site is located. The 4H11 antibody occupies the apo[a] binding site in the C-terminus of apoB (top). After the transient transfection of HEK293 cells, the PCSK9 conditioned medium was collected and concentrated. The conditioned medium was adjusted so equal amounts of PCSK9 were incubated with LDL. 4H11 decreases LDL binding demonstrating it occupies the binding site of apoB100 to apo[a]. Conversely, the BSol7 mAb does not interact in that region (apo[a] binding site), allowing LDL binding (bottom).

## 4.2 Results

To analyze the effects of mutations on PCSK9-LDL binding, equal amounts of PCSK9-G128S and PCSK9-G128R contained in the conditioned medium were incubated with isolated human LDL. Finally, LDL-bound and unbound PCSK9 were separated using the Optiprep density gradient via ultracentrifugation, as described above. A western blot was performed to analyze the LDL fraction PCSK9. This analysis showed a trend towards increased LDL binding for the G128S PCSK9 variant and no change for the G128R mutation (**Fig. 17**). However, after quantification, the G128S mediated increase in LDL binding was not statistically significant. As well, the G128R mutation did not seem to improve or worsen LDL binding in a significant way compared to WT. These results suggest that the G128 residue does not greatly affect LDL binding affinity.

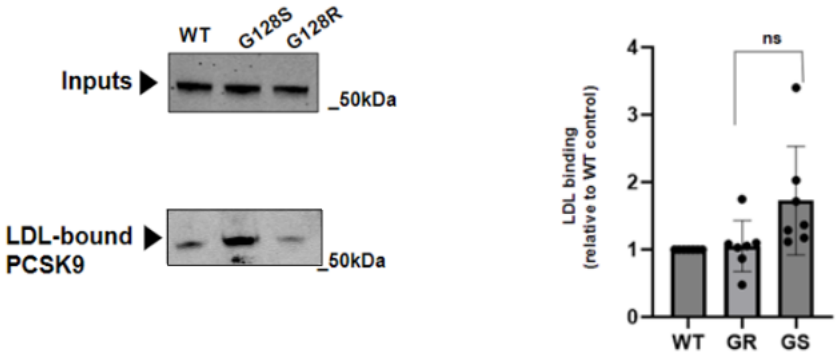


**Figure 18. G128 does not affect LDL binding.** After the transient transfection of HEK293 cells, the PCSK9 conditioned medium was collected and concentrated. The conditioned medium adjusted for equal amounts of PCSK9 was incubated with LDL. The Optiprep density gradient separated the LDL bound and unbound PCSK9, the unbound was found at the bottom of the tube.

After ultracentrifugation, the LDL fraction was removed. The PCSK9 from the LDL fraction was determined followed by a Western blot. The results from the Western blots were compared to WT and shown is a representation (n=3). Significant changes in LDL binding compared to WT-PCSK9 were determined by a one-sample t-test using GraphPad Prism 10.

## 4.3 Discussion

Although the G128 residue seems to be conserved among the species that are known to have Lp[a], variants of G128 are present in species lacking Lp[a]. We were interested to see if alterations at position 128 affect PCSK9-LDL binding affinity, as this could potentially be related to Lp[a] formation. The results suggest that there is no correlation between the two, at least in terms of the in vitro binding affinity of PCSK9 to isolated LDL. Since G128 is located between S127 and D129, which are known to play a role in PCSK9-LDL binding, a substitution in this position could alter PCSK9 conformation, reducing LDL binding affinity. However, there was no significant increase or decrease in LDL binding in G128R or G128S, suggesting these residues are not critical for LDL binding (**Fig. 17**). Although the residue at position 128 was found to have no significant effect on LDL binding under these in vitro conditions, the G128 residue may still have an undefined role in Lp[a] formation physiologically. As mentioned previously, 4H11 disrupts the binding of LDL to PCSK9 and targets the apoB100 segment responsible for the secondary apo[a] binding site. This could potentially facilitate Lp[a] formation[103]; however, our results support that this effect would not be through affecting PCSK9-LDL binding affinity. A potential next step would be to assess whether LDL binding of the truncated furin-cleaved form of PCSK9 is affected by the G128 residue. Interestingly, PCSK9i-mAbs such as alirocumab prevent the production of furin-cleaved PCSK9 by blocking the proteolysis site, which overlaps the LDLR binding region

in the PCSK9 catalytic domain. Our lab has recently found that furin-cleaved PCSK9 displays improved binding to LDL and ox-LDL. Therefore, it may be specific aspects of the furin-cleaved form of PCSK9 that facilitate apo[a] binding to LDL-apoB100 in the formation of Lp[a].

# Chapter 5: Materials and Methods

## Site mutagenesis

Site mutagenesis was used to generate a plasmid vector to produce PCSK9-Y107F, PCSK9-D129N, PCSK9-D129E, PCSK9-D129A, and PCSK9-D129G. Forward and backward primers were designed on SeqBuilder Pro 15 software to introduce point mutations into the pcDNA3.1 vector containing the WT-PCSK9 sequence. The PCR reaction used was based on the Quik-change kit (Promega). The PCR reaction is 25 µl containing 5X Phusion buffer, 10 mM dNTP mixture, forward primer (10 µM), reverse primer (10 µM), template DNA (25ng @ 10 ng/µl), Phusion DNA polymerase (2U/ul) and H2O DNAse, RNAse-free. The PCR reaction begins with the initial denaturation at 98 °C for 30 seconds. Followed by 25 cycles of the following three steps: denaturation (95 °C for 30 seconds), amplification (the temperature is set to two degrees below the hairpin temperature), and extension (72 °C for 30 seconds). The final extension is at 72 °C for 2 minutes. Following the PCR, the reaction was digested with 0.5 ul of DpnI (20U/µl) for an hour at 37 °C. The DNA was transformed into XL10 Gold ultracompetent cells and sent for sequencing to confirm the proper mutation was introduced.

## Cell culture and conditioned media:

HEK293 cells were maintained in Dulbecco Modified Eagle Medium (DMEM) (4.5 g/L glucose) supplemented with 5 mL penicillin, 50 mL FBS (fetal bovine serum), and 5 mL sodium pyruvate and kept in the incubator at 5% carbon dioxide and 37 °C. For transient transfections, cells were grown to ~70% confluency and then transiently transfected with 3.0 µg of DNA (either wildtype or mutant PCSK9 of interest) and 9.9 µl of Polyjet transfection reagent (FroggoBio) per well in 6-well cell culture dishes. The next day, cells were replaced with DMEM without FBS, ITS (insulin-

transferrin-selenium supplement – Sigma), and penicillin, allowing PCSK9 to be secreted into the medium. Two days later, the conditioned medium was collected and spun down for 5 minutes at 1000 x *g* in a 15 ml tube. The supernatant was removed from the cell debris. The supernatant was placed in a 10 kDa amicon concentrator and centrifuged for 15 minutes at 3500 rpm. The medium held back was collected, and a western blot was performed to determine the quantity by comparison to the purified PCSK9 standard.

**Western blotting**

The WCE, conditioned medium, or other proteins were heated for 10 minutes at 70 °C and loaded onto a 6-20% homemade SDS-PAGE gel or a BOLT precast gel (Thermo-Invitrogen). After the gel was run, it was electrophoretically transferred to a nitrocellulose membrane for 1 hour at 100V. The membrane was blocked with PBS and 5% skimmed milk, and primary antibodies followed by secondary antibodies (IRdye800) were used to detect the proteins targeted. These were scanned using the LICOR Odyssey infrared imaging system (LI-COR Bioscience). The results were visualized using the Odyssey 2.0 software (LI-COR Bioscience).

**In vitro PCSK9-LDL binding assay**

The concentrated conditioned medium was adjusted, and equal amounts of mutant PCSK9 were incubated with HBS-C and 100 uL of isolated human LDL ($d$=1.019-1.065 g/ml) at 37 °C for 1 hour. Following incubation, the reaction is combined with 1600 µL of 25 mM HEPES and 450 µL of 60% optiprep in 3.3 mL Beckman optiprep tubes. The tubes were filled using a 23G needle and overlayed using a 3 ml syringe of 25 mM HEPES solution. The centrifuge was run using the TLN100 rotor at 100,000 rpm for 2 hours at 4 °C. Using an optiprep gradient ultracentrifugation,

the LDL-bound and unbound PCSK9 were separated. A 22G needle was used with a 1 ml syringe, to remove 0.6 ml of the LDL band. A direct fraction (directly from the LDL fraction) was run on a western blot to analyze LDL binding.

**LDLR-dependent cell uptake**

Cell uptake was tested in LDLR-transfected HEK293 cells for the various PCSK9 mutants. HEK293 cells were maintained in Dulbecco Modified Eagle Medium (DMEM) (4.5 g/L glucose) supplemented with 5 mL penicillin, 50 mL FBS, and 5 mL sodium pyruvate and kept in the incubator at 5% carbon dioxide and 37 °C. For transient transfections, cells were grown in 100 mm dishes to ~70% confluency and then transiently transfected with 3.0 μg of DNA (LDLR and empty vector) and 9.9 μl of Polyjet per well in 6-well cell culture dishes. WT-PCSK9 or variants (D129E, D129N, D129A, or Y107F) conditioned medium was added to the cell and incubated at a physiological concentration of 3 μg/mL for 2 h in the presence of 100 μM chloroquine to prevent lysosomal degradation of internalized LDLR. The cells were harvested, and a western blot was performed using 30 μg of the WCE, probing for PCSK9, LDLR, and actin as a loading control.

**Whole cell extract**

HEK293 cells were maintained in Dulbecco Modified Eagle Medium-High (DMEM) (4.5 g/L glucose) supplemented with 5 mL penicillin, 50 mL FBS, and 5 mL sodium pyruvate was kept in the incubator at 5% carbon dioxide and 37 °C. For transient transfections, cells were grown in 100 mm dishes to ~70% confluency and then transiently transfected with 3.0 μg of DNA (LDLR and empty vector) and 9.9 μl of Polyjet per well in 6-well cell culture dishes. Two days later, the medium was aspirated, and the cells were washed twice with 2 ml of PBS-CM or TBS-C. For the

third wash, 1 ml of PBS-CM was used on the cell, a scraper was used to scrape the cells from the 6 wells, and the cells were transferred to a 1.5 mL Eppendorf tube using the 1000 µl pipette. The cells were spun for 5 minutes at 1000 x *g*, and the supernatant was removed without disturbing the cell pellet. The cell pellet was resuspended in 50 µl of Tris lysis buffer (25 mM Tris, pH 7.4, 150 mM NaCl, 1% NP-40, 5 mM EDTA, 5 mM EGTA) with supplements (1 mM DTT, 1 mM PMSF 1 mM, 1X PI cocktail (Roche)). The mixture was incubated on ice for 15-20 minutes and spun for 15-20 minutes at max speed (13 300 rpm) at 4 °C. The supernatant represents the WCE. A protein µBCA follows to determine the protein concentration.

**µBCA protein assay**

Standards and the samples were prepared in a final volume of 50 µL each. Five standards were prepared with the following concentrations of BSA: 0 µg, 4 µg, 8 µg, 16 µg, and 24 µg. Dilute 5 µL of each sample in 45 µL of dd$H_2O$. 1 mL of the solution A/B mixture was added to both standards and samples. The mixtures were incubated for 30 minutes at 37 °C, and the absorbance was measured for the samples and standards at 562 nm.

**Protein purification**

Recombinant human wild-type PCSK9 and the D129A PCSK9 mutation were produced in stable transfected HEK293S cells. The HEK293s cell line was split into 20 x 100 mm dishes using DMEM (4.5 g/L glucose) + 10% FBS, 5 ml P/S, and 5 ml sodium pyruvate. The cells were grown to ~70% confluency, washed twice with 5 ml of PBS, incubated with 1 ml of trypsin, and replaced with 5 ml of medium to remove the cells from the plate. The 5 ml of medium containing the cells from each of the 20 plates was placed into two 50 ml falcon tubes. The medium containing the

cells (described above) is added to a pot with 1000 mL of DMEM (4.5 g/L glucose), 10 ml of ITS, and 50 ml of L-glutamine. The pot is placed in the incubator for a week at 37 °C, shaking at 225 rpm. After a week, the medium was collected and filtered through a 0.22 μm filter unit, and Tris buffer pH 7.0 was added to the final concentration of 25 mM. 8–10 ml of FLAG-M2 agarose (Sigma) slurry is transferred to a small column, and 50 ml of wash buffer is run through the column. To set up the column, 2 ml of beads and 40 ml of TBS-C were run through the column, followed by a wash of 50 ml of TBS-C run through slowly to not disrupt the beads. The medium was run overnight slowly through the column, allowing the beads to capture FLAG-tagged PCSK9. The next day, the column was washed with 200 ml of TBS-C and eluted with 100 μg/ml FLAG peptide. The column was washed with 0.1 M glycine pH 3.5 buffer, followed by another wash with 20 mL TBS-C pH 7. These steps were repeated for all three bottles containing the conditioned medium. The FLAG-eluted proteins were concentrated using an Amicon Ultra concentrator (10 MW cut-off) and purified by size exclusion chromatography on a Superdex 200 column. In the Superdex 200 column, the PCSK9 peak was eluted at 8 ml, and the fractions from the main large peaks were collected (usually 7-8 fractions of 0.5 ml each). After the size exclusion, the recovered PCSK9 was concentrated again, and the concentration was determined by uBCA. The concentration was adjusted to 4 mg/ml for storage at -80oC in single-use aliquots.

**LDLR Plate-binding assay**

Maxisorp plates were coated with 10 μg/ml of purified LDLR-ECD in coating buffer (20 mM NaPO4, pH 7.5, 100 mM NaCl) 100ul per well. The plate was sealed and kept in the fridge overnight. The next morning, the wells were emptied, and the plate was washed 3x for 3 minutes each wash with 200 μl per well of the wash buffer (1x PBS and 0.08% tween-20). The wells were

emptied after every wash. The plate was coated with 200 µl per well of the blocking buffer (20 mM NaPO4 pH7.5, 100 mM NaCl, and 0.5% BSA) for an hour at room temperature. The plate was washed three times again for 3 minutes each and incubated with 100 µl per well of the sample diluent (20 mM NaPO4 pH 7.5, 100 mM NaCl, 0.5% BSA, and 0.08% Tween-20) starting at 2400 ng/ml, 1200 ng/ml, 600 ng/ml, 300 ng/ml, 150 ng/ml, 75 ng/ml, 37.5 ng/ml, and 0 ng/ml of PCSK9-WT or mutant (D129A or delt-PCSK9) for an hour at 37 °C, shaking at 600 rpm. The plate was washed again three times with the wash buffer and incubated with 100 µL per well of 10 µg/ml 1697 biotinylated Ab in blocking buffer for an hour at 37 °C, shaken at 600 rpm. The plate was washed again three times and incubated with 100 µl per well of 1:66 000 avidin HRP (200 ng/ml) in blocking buffer for an hour at 37 °C, shaken at 600 rpm. The plate was washed three times and incubated with 100 µl per well of TMB ELISA reagent (at room temperature) for 15 minutes. The colour change indicates the reaction is occurring, the wells change colour to blue. After 15 minutes, 100 uL per well of $H_2SO4$ was added, which stopped the reaction. The ELISA plate is read on the Synergy plate reader at 450 nm.

**Cellular LDLR degradation in Hepa1c1c7 assay**

For the LDLR degradation experiment, Hepa1c1c7 cells were grown in 60-nm dishes with complete medium (MEM alpha + 10% FBS + P/S). Once 60% confluent, cells were switched to sterol-depletion medium (MEM alpha, 5% NCLPPS (newborn calf lipoprotein-poor serum), P/S, melavonate (25 µM), pravastatin (10 µM)) and incubated overnight at 37°C. The next day, WT-PCSK9 or mutant variants at different concentrations (1.5 µg/ml, 2.5 µg/ml, and 5 µg/ml) without the presence of statins were added and incubated for 4 hours at 37°C. The WCE was harvested, and a western blot was performed probing for LDLR, transferrin, actin, and 15A6.

**Statistical analysis**

Statistical analyses involved a column statistics analysis with a one-sample t-test to compare mutants to the WT-PCSK9 control. Statistical significance was relevant if $p < 0.05$. All statistical analyses and graphs were done using GraphPad Prism 10.0 software.

## Chapter 6: Conclusion and further studies

This dissertation seeks to further understand PCSK9 function, more specifically elucidating the autoinhibitory effects of PCSK9's prodomain and its role in Lp[a] formation. These studies further define the PCSK9-LDL binding site and inform on the mechanisms of action of several GOF mutations in the prodomain. Nonetheless, some information from the following topics can be further explored:

**PCSK9 prodomain's role in autoinhibition.** The D129 residue is located in proximity to the S127 residue and the IDR, both of which are known to affect LDLR binding. These findings suggest that any mutation at the D129 position impacts LDLR binding affinity. Mutations such as D129A also seem to affect LDLR degradation on the cell surface. These results indicate the D129 residue could be involved in an intramolecular interaction that lowers PCSK9-LDLR binding affinity. Additionally, the D129 residue seems to have a similar effect on LDLR binding and degradation as the S127 and the IDR, implying that due to the residue's location in the prodomain, it could contribute to the autoinhibitory effect. In terms of LDL binding, any substitution at this position abolishes LDL binding. Therefore, D129 could potentially interact directly with apoB100 on LDL or could maintain PCSK9 conformation, allowing its interaction with LDL. These studies highlight the relevance of the D129 residue in cholesterol metabolism due to its significant impact on LDLR binding and LDL binding. Future investigations should focus on the effects of D129 mutations added to the del53-PCSK9 plasmid to determine if the effects are redundant or additive and further understand the mechanisms of PCSK9-mediated LDLR degradation and the role of the IDR autoinhibition.

**PCSK9 and HSPGs.** The GOF mutations R105W and R96L in PCSK9 have been identified to cause hypercholesterolemia and are located in the HSPG arginine binding region. However, these mutations act through different mechanisms. The R105W mutation greatly lowered LDL binding, further supporting that LDL and HSPG share a binding site. Therefore, since R105W decreases LDL binding, more PCSK9 is unbound from LDL and available to bind the LDLR. Furthermore, these results show a single mutation can affect LDL binding, but a single mutation in PCSK9 doesn't decrease its binding to HSPGs since many arginine residues are responsible for this cumulative binding. As for R96L, the mutation maintains LDL binding, which may impact another mechanism by potentially causing a conformational change affecting the IDR positioning and reducing the IDR's autoinhibition effect. Further studies determining how R96L induces a conformational change in PCSK9 focusing on its interaction with the IDR are necessary.

**PCSK9 in Lp[a] formation.** Even though the G128 residues are conserved in species known to have Lp[a], species lacking Lp[a] lack the presence of G128. The findings from these studies suggest that there is no correlation between the G128 residue and Lp[a] formation. This implies that G128 may not be important in LDL binding and Lp[a] formation. We anticipated a decrease in LDL binding would be observed in species lacking Lp[a] compared to WT-PCSK9 since it's hypothesized that PCSK9 holds apoB in a conformation favourable for apo[a] binding. Therefore, species lacking Lp[a] would not require PCSK9 to fulfill that role, leading to lower binding affinity to LDL. A future direction for this study would be to investigate the impact of furin-cleaved PCSK9 on LDL binding. Alirocumab inhibits furin cleavage of PCSK9 and decreases Lp[a] formation, but it remains unexplored whether these effects are related. Exploring furin-cleaved

PCSK9 and its role in Lp[a] formation is necessary since furin-cleaved PCSK9 improves LDL and ox-LDL binding; it may stabilize LDL-apoB100 in a favourable conformation for apo[a] binding.

**Conclusion.** This dissertation provided further insight into the structure/function of PCSK9's prodomain. The introduction of GOF mutations in the PCSK9s prodomain helped in the identification of residues involved in LDL binding, further characterizing the PCSK9-LDL binding site. However, the autoinhibitory effects of the IDR in PCSK9 remain undefined, especially its mechanism of action. A supplemental understanding of the autoinhibition mechanism could lead to new therapeutic strategies targeting PCSK9 in various diseases such as hypercholesterolemia. As for function, this thesis investigated PCSK9's role in lipoprotein metabolism. Since much is still unknown about Lp[a] and how PCSK9i-mAbs reduce Lp[a] levels, this suggests that PCSK9-LDL binding could be targeted to lower Lp[a] levels. Further investigation into PCSK9's role in Lp[a] formation could help develop a therapeutical approach that reduces the risk of a cardiovascular event.

## References:


[1] Sarkar, S. K., Matyas, A., Asikhia, I., Hu, Z., Golder, M., Beehler, K., Kosenko, T., & Lagace, T. A. (2022). Pathogenic gain-of-function mutations in the prodomain and C-terminal domain of PCSK9 inhibit LDL binding. *Frontiers in Physiology*, *13*. https://doi.org/10.3389/fphys.2022.960272

[2] Seidah, N. G. (2019). The elusive inhibitory function of the acidic N-terminal segment of the prodomain of PCSK9: The plot thickens. *Journal of Molecular Biology*, *431*(5), 904–907. https://doi.org/10.1016/j.jmb.2019.01.015

[3] Sarkar, S. K., Foo, A. C. Y., Matyas, A., Asikhia, I., Kosenko, T., Goto, N. K., Vergara-Jaque, A., & Lagace, T. A. (2020). A transient amphipathic helix in the prodomain of PCSK9 facilitates binding to low-density lipoprotein particles. *Journal of Biological Chemistry*, *295*(8), 2285–2298. https://doi.org/10.1074/jbc.ra119.010221

[4] Galvan, A. M., & Chorba, J. S. (2019). Cell-associated heparin-like molecules modulate the ability of LDL to regulate PCSK9 uptake. *Journal of Lipid Research*, *60*(1), 71–84. https://doi.org/10.1194/jlr.m087189

[5] Homer, V. M., Marais, A. D., Charlton, F., Laurie, A. D., Hurndell, N., Scott, R., Mangili, F., Sullivan, D. R., Barter, P. J., Rye, K.-A., George, P. M., & Lambert, G. (2008). Identification and characterization of two non-secreted PCSK9 mutants associated with familial hypercholesterolemia in cohorts from New Zealand and South Africa. *Atherosclerosis*, *196*(2), 659–666. https://doi.org/10.1016/j.atherosclerosis.2007.07.022

[6] Benjannet, S., Rhainds, D., Essalmani, R., Mayne, J., Wickham, L., Jin, W., Asselin, M.-C., Hamelin, J., Varret, M., Allard, D., Trillard, M., Abifadel, M., Tebon, A., Attie, A. D., Rader, D. J., Boileau, C., Brissette, L., Chrétien, M., Prat, A., & Seidah, N. G. (2004a). NARC-1/PCSK9 and its natural mutants. *Journal of Biological Chemistry*, *279*(47), 48865–48875. https://doi.org/10.1074/jbc.m409699200

[7] Pejic, R. N. (2014). *Familial hypercholesterolemia*. Ochsner journal. https://www.ncbi.nlm.nih.gov/pmc/articles/PMC4295745/

[8] Rafieian-Kopaei, M., Setorki, M., Doudi, M., Baradaran, A., & Nasri, H. (2014, August). *Atherosclerosis: Process, indicators, risk factors and new hopes*. International journal of preventive medicine. https://www.ncbi.nlm.nih.gov/pmc/articles/PMC4258672/

[9] Cockerill, G. (1970, January 1). *Atherosclerosis*. Mechanisms of Vascular Disease: A Reference Book for Vascular Specialists [Internet]. https://www.ncbi.nlm.nih.gov/books/NBK534258/

[10]Linton, M. F. (2019, January 3). *The role of lipids and lipoproteins in atherosclerosis*. Endotext [Internet].

https://www.ncbi.nlm.nih.gov/books/NBK343489/#:~:text=The%20response%20to%20retention%20hypothesis,particles%20that%20initiate%20inflammatory%20responses

[11]Gui, Y., Zheng, H., & Cao, R. Y. (2022). Foam cells in atherosclerosis: Novel insights into its origins, consequences, and molecular mechanisms. *Frontiers in Cardiovascular Medicine*, *9*. https://doi.org/10.3389/fcvm.2022.845942

[12] Lu, Y., Cui, X., Zhang, L., Wang, X., Xu, Y., Qin, Z., Liu, G., Wang, Q., Tian, K., Lim, K. S., Charles, C. J., Zhang, J., & Tang, J. (2022). The functional role of lipoproteins in atherosclerosis: Novel directions for diagnosis and targeting therapy. *Aging and Disease*, *13*(2), 491. https://doi.org/10.14336/ad.2021.0929

[13] Lambert, G., Sjouke, B., Choque, B., Kastelein, J. J. P., & Hovingh, G. K. (2012). The PCSK9 Decade. *Journal of Lipid Research*, *53*(12), 2515–2524. https://doi.org/10.1194/jlr.r026658

[14] Dron, J. S., & Hegele, R. A. (2017a). Complexity of mechanisms among human proprotein convertase subtilisin–kexin type 9 variants. *Current Opinion in Lipidology*, *28*(2), 161–169. https://doi.org/10.1097/mol.0000000000000386

[15] Kent, S. T., Rosenson, R. S., Avery, C. L., Chen, Y.-D. I., Correa, A., Cummings, S. R., Cupples, L. A., Cushman, M., Evans, D. S., Gudnason, V., Harris, T. B., Howard, G., Irvin, M. R., Judd, S. E., Jukema, J. W., Lange, L., Levitan, E. B., Li, X., Liu, Y., … Muntner, P. (2017). *pcsk9* loss-of-function variants, low-density lipoprotein cholesterol, and risk of coronary heart disease and stroke. *Circulation: Cardiovascular Genetics*, *10*(4). https://doi.org/10.1161/circgenetics.116.001632

[16] Bayona, A., Arrieta, F., Rodríguez-Jiménez, C., Cerrato, F., Rodríguez-Nóvoa, S., Fernández-Lucas, M., Gómez-Coronado, D., & Mata, P. (2020a). Loss-of-function mutation of PCSK9 as a protective factor in the clinical expression of familial hypercholesterolemia. *Medicine*, *99*(34). https://doi.org/10.1097/md.0000000000021754

[17] Lebeau, P. F., Platko, K., Byun, J. H., Makda, Y., & Austin, R. C. (2022). The emerging roles of intracellular PCSK9 and their implications in endoplasmic reticulum stress and Metabolic Diseases. *Metabolites*, *12*(3), 215. https://doi.org/10.3390/metabo12030215

[18] Feingold KR. Cholesterol Lowering Drugs. [Updated 2021 Mar 30]. In: Feingold KR, Anawalt B, Boyce A, et al., editors. Endotext [Internet]. South Dartmouth (MA): MDText.com, Inc.; 2000-. Available from: https://www.ncbi.nlm.nih.gov/books/NBK395573

[19] Sizar, O. (2024, February 29). *Statin medications*. StatPearls [Internet]. https://www.ncbi.nlm.nih.gov/books/NBK430940/

[20] Sun, L., Wolska, A., Amar, M., Zubirán, R., & Remaley, A. T. (2023). Approach to the patient with a suboptimal statin response: Causes and algorithm for Clinical Management. *The Journal*

*of Clinical Endocrinology & Metabolism*, *108*(9), 2424–2434. https://doi.org/10.1210/clinem/dgad153

[21] Dong, B., Wu, M., Li, H., Kraemer, F. B., Adeli, K., Seidah, N. G., Park, S. W., & Liu, J. (2010). Strong induction of PCSK9 gene expression through HNF1A and SREBP2: Mechanism for the resistance to LDL-cholesterol lowering effect of statins in dyslipidemic hamsters. *Journal of Lipid Research*, *51*(6), 1486–1495. https://doi.org/10.1194/jlr.m003566

[22] Paciullo F, Momi S, and Gresele P. PCSK9 in Haemostasis and Thrombosis: Possible Pleiotropic Effects of PCSK9 Inhibitors in Cardiovascular Prevention. Thromb Haemost. 2019;119(3):359-67.

[23] Kwon HJ, Lagace TA, McNutt MC, Horton JD, and Deisenhofer J. Molecular basis for LDL receptor recognition by PCSK9. *Proc Natl Acad Sci U S A.* 2008;105(6):1820-5.

[24] Chan JC, Piper DE, Cao Q, Liu D, King C, Wang W, et al. A proprotein convertase subtilisin/kexin type 9 neutralizing antibody reduces serum cholesterol in mice and nonhuman primates. *Proc Natl Acad Sci U S A.* 2009.

[25] Ko DT, Khan AM, Kotrri G, Austin PC, Wijeysundera HC, Koh M, et al. Eligibility, Clinical Outcomes, and Budget Impact of PCSK9 Inhibitor Adoption: The CANHEART PCSK9 Study. *J Am Heart Assoc.* 2018;7(21):e010007.

[26] *Ezetimibe*. HEART UK - The Cholesterol Charity. (n.d.). https://www.heartuk.org.uk/getting-treatment/ezetimibe#:~:text=Ezetimibe can lower LDL cholesterol,the dose of the statin.

[27] Rakocevic, J., Dobric, M., Vucic, R., Furtula, M., Zaletel, I., Milutinovic, K., Ilijevski, A., Borovic, M. L., Tomasevic, M., & Bajcetic, M. (2023). Small interfering ribonucleic acid as lipid-lowering therapy: Inclisiran in Focus. *International Journal of Molecular Sciences*, *24*(6), 6012. https://doi.org/10.3390/ijms24066012

[28] Liu, C., Chen, J., Chen, H., Zhang, T., He, D., Luo, Q., Chi, J., Hong, Z., Liao, Y., Zhang, S., Wu, Q., Cen, H., Chen, G., Li, J., & Wang, L. (2022). PCSK9 inhibition: From current advances to evolving future. *Cells*, *11*(19), 2972. https://doi.org/10.3390/cells11192972

[29] Fasano, T., Sun, X.-M., Patel, D. D., & Soutar, A. K. (2009). Degradation of LDLR protein mediated by 'gain of function' PCSK9 mutants in normal and Arh Cells. *Atherosclerosis*, *203*(1), 166–171. https://doi.org/10.1016/j.atherosclerosis.2008.10.027

[30] McNutt, M. C., Lagace, T. A., & Horton, J. D. (2007). Catalytic activity is not required for secreted PCSK9 to reduce low density lipoprotein receptors in hepg2 cells. *Journal of Biological Chemistry*, *282*(29), 20799–20803. https://doi.org/10.1074/jbc.c700095200

[31] Schulz, R., & Schlüter, K.-D. (2017). PCSK9 targets important for lipid metabolism. *Clinical Research in Cardiology Supplements*, *12*(S1), 2–11. https://doi.org/10.1007/s11789-017-0085-0

[32] SEIDAH, N., MAYER, G., ZAID, A., ROUSSELET, E., NASSOURY, N., POIRIER, S., ESSALMANI, R., & PRAT, A. (2008). The activation and physiological functions of the proprotein convertases. *The International Journal of Biochemistry & Cell Biology*, *40*(6–7), 1111–1125. https://doi.org/10.1016/j.biocel.2008.01.030

[33] Seidah, N. G., Sadr, M. S., Chrétien, M., & Mbikay, M. (2013). The multifaceted proprotein convertases: Their unique, redundant, complementary, and opposite functions. *Journal of Biological Chemistry*, *288*(30), 21473–21481. https://doi.org/10.1074/jbc.r113.481549

[34] Lakoski SG, Lagace TA, Cohen JC, Horton JD, and Hobbs HH. Genetic and metabolic determinants of plasma PCSK9 levels. *J Clin Endocrinol Metab.* 2009;94(7):2537-43

[35] Steiner, D. F. (1998). The proprotein convertases. *Current Opinion in Chemical Biology*, *2*(1), 31–39. https://doi.org/10.1016/s1367-5931(98)80033-1

[36] Seidah, N. G., & Prat, A. (2012). The biology and therapeutic targeting of the proprotein convertases. *Nature Reviews Drug Discovery*, *11*(5), 367–383. https://doi.org/10.1038/nrd3699

[37] Cunningham, D., Danley, D. E., Geoghegan, K. F., Griffor, M. C., Hawkins, J. L., Subashi, T. A., Varghese, A. H., Ammirati, M. J., Culp, J. S., Hoth, L. R., Mansour, M. N., McGrath, K. M., Seddon, A. P., Shenolikar, S., Stutzman-Engwall, K. J., Warren, L. C., Xia, D., & Qiu, X. (2007). Structural and biophysical studies of PCSK9 and its mutants linked to familial hypercholesterolemia. *Nature Structural & Molecular Biology*, *14*(5), 413–419. https://doi.org/10.1038/nsmb1235

[38] Seidah NG, Benjannet S, Wickham L, Marcinkiewicz J, Jasmin SB, Stifani S, et al. The secretory proprotein convertase neural apoptosis-regulated convertase 1 (NARC-1): liver regeneration and neuronal differentiation. *Proc Natl Acad Sci U S A.* 2003;100(3):928-33

[39] Seidah, N. G. (2021). The PCSK9 discovery, an inactive protease with varied functions in hypercholesterolemia, viral infections, and cancer. Journal of Lipid Research, 62, 100130. https://doi.org/10.1016/j.jlr.2021.100130

[40] Fruchart Gaillard, C., Ouadda, A. B., Ciccone, L., Girard, E., Mikaeeli, S., Evagelidis, A., Le Dévéhat, M., Susan-Resiga, D., Lajeunesse, E. C., Nozach, H., Ramos, O. H., Thureau, A., Legrand, P., Prat, A., Dive, V., & Seidah, N. G. (2023). Molecular interactions of PCSK9 with an inhibitory nanobody, CAP1 and HLA-C: Functional regulation of LDLR levels. *Molecular Metabolism*, *67*, 101662. https://doi.org/10.1016/j.molmet.2022.101662

[41] Zhang D-W, Lagace TA, Garuti R, Zhao Z, McDonald M, Horton JD, et al. Binding of proprotein convertase subtilisin/kexin type 9 to epidermal growth factor-like repeat A of low density lipoprotein receptor decreases receptor recycling and increases degradation. *J Biol Chem* 2007;282(25):18602-12

[42] Peterson, A. S., Fong, L. G., & Young, S. G. (2008). PCSK9 function and physiology. *Journal of Lipid Research*, *49*(6), 1152–1156. https://doi.org/10.1194/jlr.e800008-jlr200

[43] Xia, X., Peng, Z., Gu, H., Wang, M., Wang, G., & Zhang, D. (2021). Regulation of PCSK9 expression and function: Mechanisms and therapeutic implications. *Frontiers in Cardiovascular Medicine*, *8*. https://doi.org/10.3389/fcvm.2021.764038

[44] Seidah, N. G., & Prat, A. (2021). The multifaceted biology of PCSK9. *Endocrine Reviews*, *43*(3), 558–582. https://doi.org/10.1210/endrev/bnab035

[45] Hampton EN, Knuth MW, Li J, Harris JL, Lesley SA, and Spraggon G. The self-inhibited structure of full-length PCSK9 at 1.9 A reveals structural homology with resistin within the C-terminal domain. *Proc Natl Acad Sci U S A.* 2007;104(37):14604-9.

[46] Cunningham D, Danley DE, Geoghegan KF, Griffor MC, Hawkins JL, Subashi TA, et al. Structural and biophysical studies of PCSK9 and its mutants linked to familial hypercholesterolemia. *Nat Struct Mol Biol.* 2007;14(5):413-9.

[47] Lagace TA, Curtis DE, Garuti R, McNutt MC, Park SW, Prather HB, et al. Secreted PCSK9 decreases the number of LDL receptors in hepatocytes and in livers of parabiotic mice. *J Clin Invest.* 2006;116(11):2995-3005.

[48] Cunningham, D., Danley, D. E., Geoghegan, K. F., Griffor, M. C., Hawkins, J. L., Subashi, T. A., Varghese, A. H., Ammirati, M. J., Culp, J. S., Hoth, L. R., Mansour, M. N., McGrath, K. M., Seddon, A. P., Shenolikar, S., Stutzman-Engwall, K. J., Warren, L. C., Xia, D., & Qiu, X. (2007a). Structural and biophysical studies of PCSK9 and its mutants linked to familial hypercholesterolemia. *Nature Structural & Molecular Biology*, *14*(5), 413–419. https://doi.org/10.1038/nsmb1235

[49] Guo, Q., Feng, X., & Zhou, Y. (2020). PCSK9 variants in familial hypercholesterolemia: A comprehensive synopsis. *Frontiers in Genetics*, *11*. https://doi.org/10.3389/fgene.2020.01020

[50] Huang, S., Henry, L., Ho, Y. K., Pownall, H. J., & Rudenko, G. (2010). Mechanism of LDL binding and release probed by structure-based mutagenesis of the LDL receptor. *Journal of Lipid Research*, *51*(2), 297–308. https://doi.org/10.1194/jlr.m000422

[51] Horton JD, Goldstein JL, and Brown MS. SREBPs:activators of the complete program of cholesterol and fatty acid synthesis in the liver. *J Clin Invest.* 2002;109(9):1125-31

[52] Islam, M. M., Hlushchenko, I., & Pfisterer, S. G. (2022). Low-density lipoprotein internalization, degradation and receptor recycling along membrane contact sites. *Frontiers in Cell and Developmental Biology*, *10*. https://doi.org/10.3389/fcell.2022.826379

[53] Piper DE, Jackson S, Liu Q, Romanow WG, Shetterly S, Thibault ST, et al. The crystal structure of PCSK9: A regulator of plasma LDL-cholesterol. *Structure.* 2007;15(5):545-52.

[54] Lagace, T. A. (2014). PCSK9 and LDLR degradation. *Current Opinion in Lipidology*, *25*(5), 387–393. https://doi.org/10.1097/mol.0000000000000114

[55] Martin, W. R., Lightstone, F. C., & Cheng, F. (2020). In silico insights into protein–protein interaction disruptive mutations in the PCSK9-LDLR complex. *International Journal of Molecular Sciences*, *21*(5), 1550. https://doi.org/10.3390/ijms21051550

[56] Gustafsen, C., Olsen, D., Vilstrup, J., Lund, S., Reinhardt, A., Wellner, N., Larsen, T., Andersen, C. B., Weyer, K., Li, J., Seeberger, P. H., Thirup, S., Madsen, P., & Glerup, S. (2017). Heparan sulfate proteoglycans present PCSK9 to the LDL receptor. *Nature Communications*, *8*(1). https://doi.org/10.1038/s41467-017-00568-7

[57] Poirier, S., Mayer, G., Benjannet, S., Bergeron, E., Marcinkiewicz, J., Nassoury, N., Mayer, H., Nimpf, J., Prat, A., & Seidah, N. G. (2008). The proprotein convertase PCSK9 induces the degradation of low density lipoprotein receptor (LDLR) and its closest family members VLDLR and apoer2. *Journal of Biological Chemistry*, *283*(4), 2363–2372. https://doi.org/10.1074/jbc.m708098200

[58] Gu, H., Adijiang, A., Mah, M., & Zhang, D. (2013). Characterization of the role of EGF-A of low density lipoprotein receptor in PCSK9 binding. *Journal of Lipid Research*, *54*(12), 3345–3357. https://doi.org/10.1194/jlr.m041129

[59] Somanathan, S., Jacobs, F., Wang, Q., Hanlon, A. L., Wilson, J. M., & Rader, D. J. (2014). Aav vectors expressing LDLR gain-of-function variants demonstrate increased efficacy in mouse models of familial hypercholesterolemia. *Circulation Research*, *115*(6), 591–599. https://doi.org/10.1161/circresaha.115.304008

[60] Seidah, N. G., Awan, Z., Chrétien, M., & Mbikay, M. (2014). PCSK9. *Circulation Research*, *114*(6), 1022–1036. https://doi.org/10.1161/circresaha.114.301621

[61] Brown MS, and Goldstein JL. Cholesterol feedback: from Schoenheimer's bottle to Scap's MELADL. *J Lipid Res.* 2009;50 Suppl:S15-27.

[62] Erkner, E., Hentrich, T., Schairer, R., Fitzel, R., Secker-Grob, K.-A., Jeong, J., Keppeler, H., Korkmaz, F., Schulze-Hentrich, J. M., Lengerke, C., Schneidawind, D., & Schneidawind, C. (2023, November 29). *The RORɣ/SREBP2 pathway is a master regulator of cholesterol metabolism and serves as potential therapeutic target in T(4;11) leukemia*. Nature News. https://www.nature.com/articles/s41388-023-02903-3

[63] Horton JD, Shah NA, Warrington JA, Anderson NN, Park SW, Brown MS, et al. Combined analysis of oligonucleotide microarray data from transgenic and knockout mice identifies direct SREBP target genes. *Proc Natl Acad Sci U S A.* 2003;100(21):12027-32.

[64]Brown MS, and Goldstein JL. Lowering plasma cholesterol by raising LDL receptors. *N Engl J Med.* 1981;305(9):515-7.

[65] Persson L, Cao G, Stahle L, Sjoberg BG, Troutt JS, Konrad RJ, et al. Circulating proprotein convertase subtilisin kexin type 9 has a diurnal rhythm synchronous with cholesterol synthesis and is reduced by fasting in humans. *Arterioscler Thromb Vac Biol.* 2010;30(12):2666-72.

[66] Browning JD, and Horton JD. Fasting reduces plasma proprotein convertase, subtilisin/kexin type 9 and cholesterol biosynthesis in humans. *J Lipid Res.* 2010;51(11):3359-63.

[67] Li, H., Dong, B., Park, S. W., Lee, H.-S., Chen, W., & Liu, J. (2009). Hepatocyte nuclear factor 1A plays a critical role in PCSK9 gene transcription and regulation by the natural hypocholesterolemic compound berberine. *Journal of Biological Chemistry*, *284*(42), 28885–28895. https://doi.org/10.1074/jbc.m109.052407

[68] Armendariz, A. D., & Krauss, R. M. (2009). Hepatic nuclear factor 1-α: Inflammation, genetics, and atherosclerosis. *Current Opinion in Lipidology*, *20*(2), 106–111. https://doi.org/10.1097/mol.0b013e3283295ee9

[69] *Dong B, Wu M, Li H, et al. Strong induction of PCSK9 gene expression through HNF1alpha and SREBP2: mechanism for the resistance to LDLcholesterol lowering effect of statins in dyslipidemic hamsters. J Lipid Res 2010; 51:1486–1495.*

[70] Rader, D. J. (1970, January 1). *Lipoprotein metabolism*. SpringerLink. https://link.springer.com/referenceworkentry/10.1007/978-3-540-38918-7_190

[71] Feingold, K. R. (2024, January 14). *Introduction to lipids and Lipoproteins*. Endotext [Internet]. https://www.ncbi.nlm.nih.gov/books/NBK305896/

[72] Lent-Schochet, D. (2023, January 16). *Biochemistry, lipoprotein metabolism*. StatPearls [Internet]. https://www.ncbi.nlm.nih.gov/books/NBK553193/

[73]Qiao, Y.-N., Zou, Y.-L., & Guo, S.-D. (2022). Low-density lipoprotein particles in atherosclerosis. *Frontiers in Physiology*, *13*. https://doi.org/10.3389/fphys.2022.931931

[74] *Overview of lipid metabolism - overview of lipid metabolism*. Merck Manual Professional Edition. (n.d.). https://www.merckmanuals.com/professional/endocrine-and-metabolic-disorders/lipid-disorders/overview-of-lipid-metabolism

[75] Boffa, M. B., & Koschinsky, M. L. (2022). Understanding the ins and outs of lipoprotein (a) metabolism. *Current Opinion in Lipidology*, *33*(3), 185–192. https://doi.org/10.1097/mol.0000000000000823

[76] Raal FJ, Giugliano RP, Sabatine MS, Koren MJ, Langslet G, Bays H, et al. Reduction in lipoprotein(a) with PCSK9 monoclonal antibody evolocumab (AMG 145): a pooled analysis of more than 1,300 patients in 4 phase II trials. *J Am Coll Cardiol.* 2014;63(13):1278-88

[77] Plasma lipoproteins: Apolipoprotein structure and function. (n.d.-a). https://www.jlr.org/article/S0022-2275(20)34443-6/pdf

[78] Kounatidis, D., Vallianou, N. G., Poulaki, A., Evangelopoulos, A., Panagopoulos, F., Stratigou, T., Geladari, E., Karampela, I., & Dalamaga, M. (2024). APOB100 and atherosclerosis: What's new in the 21st century? Metabolites, 14(2), 123. https://doi.org/10.3390/metabo14020123

[79] Behbodikhah, J., Ahmed, S., Elyasi, A., Kasselman, L. J., De Leon, J., Glass, A. D., & Reiss, A. B. (2021). Apolipoprotein B and cardiovascular disease: Biomarker and potential therapeutic target. *Metabolites*, *11*(10), 690. https://doi.org/10.3390/metabo11100690

[80] Milne R, Théolis R, Jr., Maurice R, Pease RJ, Weech PK, Rassart E, et al. The use of monoclonal antibodies to localize the low density lipoprotein receptor-binding domain of apolipoprotein B. *J Biol Chem.* 1989;264(33):19754-60.

[81] Devaraj, S. (2023, May 14). *Biochemistry, apolipoprotein B*. StatPearls [Internet]. https://www.ncbi.nlm.nih.gov/books/NBK538139/

[82] Elmore, B. O., Triplett, K. D., & Hall, P. R. (2015). Apolipoprotein B48, the structural component of Chylomicrons, is sufficient to antagonize Staphylococcus aureus quorum-sensing. *PLOS ONE*, *10*(5). https://doi.org/10.1371/journal.pone.0125027

[83]Lo, C. C., & Coschigano, K. T. (2020). APOB48 as an efficient regulator of intestinal lipid transport. *Frontiers in Physiology*, *11*. https://doi.org/10.3389/fphys.2020.00796

[84] Purcell-Huynh, D. A., Farese, R. V., Johnson, D. F., Flynn, L. M., Pierotti, V., Newland, D. L., Linton, M. F., Sanan, D. A., & Young, S. G. (1995). Transgenic mice expressing high levels of human apolipoprotein B develop severe atherosclerotic lesions in response to a high-fat diet. *Journal of Clinical Investigation*, *95*(5), 2246–2257. https://doi.org/10.1172/jci117915

[85] Lo, C. C., & Coschigano, K. T. (2020). APOB48 as an efficient regulator of intestinal lipid transport. *Frontiers in Physiology*, *11*. https://doi.org/10.3389/fphys.2020.00796

[86] Nakajima K;Nagamine T;Fujita MQ;Ai M;Tanaka A;Schaefer E; (n.d.). *Apolipoprotein B-48: A unique marker of Chylomicron metabolism*. Advances in clinical chemistry. https://pubmed.ncbi.nlm.nih.gov/24938018/

[87]Venugopal, S. K. (2023, April 17). *Biochemistry, low density lipoprotein*. StatPearls [Internet]. https://www.ncbi.nlm.nih.gov/books/NBK500010/#:~:text=LDL%20is%20the%20predominant%20carrier%20of%20serum%20cholesterol,and%20FC%29%20and%20displays%20beta%20mobility%20on%20electrophoresis.

[88] Dallinga-Thie GM, Franssen R, Mooij HL, Visser ME, Hassing HC, Peelman F, et al. The metabolism of triglyceride-rich lipoproteins revisited: new players, new insight. *Atherosclerosis.* 2010;211(1):1-8.

[89] Kita T, Brown MS, Bilheimer DW, and Goldstein JL. Delayed clearance of very low density and intermediate density lipoproteins with enhanced conversion to low density lipoprotein in WHHL rabbits. *Proceedings of the National Academy of Sciences of the United States of America.* 1982;79(18):5693-7.

[90] Kosenko, T., Golder, M., Leblond, G., Weng, W., and Lagace, T. A. (2013). Low density lipoprotein binds to proprotein convertase subtilisin/kexin type-9 (PCSK9) in human plasma and inhibits PCSK9-mediated low density lipoprotein receptor degradation. J. Biol. Chem. 288 (12), 8279–8288. doi:10.1074/jbc.M112.421370

[91] Watts GF, Chan DC, Dent R, Somaratne R, Wasserman SM, Scott R, Burrows S, PH RB. Factorial Effects of Evolocumab and Atorvastatin on Lipoprotein Metabolism. Circulation 2017;135(4):338-351

[92] Guardiola M, Plana N, Ibarretxe D, Cabre A, Gonzalez M, Ribalta J, Masana L. Circulating PCSK9 levels are positively correlated with NMR-assessed atherogenic dyslipidaemia in patients with high cardiovascular risk. Clin Sci (Lond) 2015;128(12):877-82

[93] Tavori H, Fan D, Blakemore JL, Yancey PG, Ding L, Linton MF, et al. Serum proprotein convertase subtilisin/kexin type 9 and cell surface low-density lipoprotein receptor: evidence for a reciprocal regulation. *Circulation.* 2013;127(24):2403-13.

[94] Wright PE, and Dyson HJ. Intrinsically disordered proteins in cellular signalling and regulation. *Nature reviews Molecular cell biology.* 2015;16(1):18-29.

[95] Sun, X.-M., Eden, E. R., Tosi, I., Neuwirth, C. K., Wile, D., Naoumova, R. P., & Soutar, A. K. (2005). Evidence for effect of mutant PCSK9 on apolipoprotein B secretion as the cause of unusually severe dominant hypercholesterolaemia. *Human Molecular Genetics*, *14*(9), 1161–1169. https://doi.org/10.1093/hmg/ddi128

[96] Mikaeeli, S., Susan-Resiga, D., Girard, E., Ben Djoudi Ouadda, A., Day, R., Prost, S., & Seidah, N. G. (2019). Functional analysis of natural PCSK9 mutants in modern and archaic humans. *The FEBS Journal*, *287*(3), 515–528. https://doi.org/10.1111/febs.15036

[97] O'Donoghue, M. L., Fazio, S., Giugliano, R. P., Stroes, E. S. G., Kanevsky, E., Gouni-Berthold, I., Im, K., Lira Pineda, A., Wasserman, S. M., Češka, R., Ezhov, M. V., Jukema, J. W., Jensen, H. K., Tokgözoğlu, S. L., Mach, F., Huber, K., Sever, P. S., Keech, A. C., Pedersen, T. R., & Sabatine, M. S. (2019). Lipoprotein(a), PCSK9 inhibition, and cardiovascular risk. *Circulation*, *139*(12), 1483–1492. https://doi.org/10.1161/circulationaha.118.037184

[98] Stein EA, and Raal FJ. Insights into PCSK9, low-density lipoprotein receptor, and low-density lipoprotein cholesterol metabolism: of mice and man. *Circulation.* 2013;127(24):2372-4.

[99] Vinci, P., Di Girolamo, F. G., Panizon, E., Tosoni, L. M., Cerrato, C., Pellicori, F., Altamura, N., Pirulli, A., Zaccari, M., Biasinutto, C., Roni, C., Fiotti, N., Schincariol, P., Mangogna, A., & Biolo, G. (2023). Lipoprotein(a) as a risk factor for cardiovascular diseases: Pathophysiology

and treatment perspectives. *International Journal of Environmental Research and Public Health*, *20*(18), 6721. https://doi.org/10.3390/ijerph20186721

[100] Gencer, B., Kronenberg, F., Stroes, E. S., & Mach, F. (2017). Lipoprotein(a): The Revenant. *European Heart Journal*, *38*(20), 1553–1560. https://doi.org/10.1093/eurheartj/ehx033

[101] Watts GF, Chan DC, Somaratne R, Wasserman SM, Scott R, Marcovina SM, et al. Controlled study of the effect of proprotein convertase subtilisin-kexin type 9 inhibition with evolocumab on lipoprotein(a) particle kinetics. *Eur Heart J.* 2018;39(27):2577-85

[102] Villard, E. F., Thedrez, A., Blankenstein, J., Croyal, M., Tran, T.-T.-T., Poirier, B., Le Bail, J.-C., Illiano, S., Nobécourt, E., Krempf, M., Blom, D. J., Marais, A. D., Janiak, P., Muslin, A. J., Guillot, E., & Lambert, G. (2016). PCSK9 modulates the secretion but not the cellular uptake of lipoprotein(a) ex vivo. *JACC: Basic to Translational Science*, *1*(6), 419–427. https://doi.org/10.1016/j.jacbts.2016.06.006

[103] Wang, X., Pease, R., Bertinato, J., & Milne, R. W. (2000). Well-defined regions of apolipoprotein B-100 undergo conformational change during its intravascular metabolism. *Arteriosclerosis, Thrombosis, and Vascular Biology*, *20*(5), 1301–1308. https://doi.org/10.1161/01.atv.20.5.1301